Sugimoto T, Ishikawa Y, Yoshimoto T, Hayashi N, Fujimoto J, Nakanishi K (2004) Interleukin 18 acts on memory T helper cells type 1 to induce airway inflammation and hyperresponsiveness in a naive host mouse. J Exp Med 199:535–545

Szabo SJ, Kim ST, Costa GL, Zhang X, Fathman CG, Glimcher LH (2000) A novel transcription factor, T-bet, directs Th1 lineage commitment. Cell 100:655–669

Szczeklik A (1988) Aspirin-induced asthma as a viral disease. Clin Allergy 18:15–20

Szczeklik A, Stevenson DD (1999) Aspirin-induced asthma: advances in pathogenesis and management. J Allergy Clin Immunol 104:5–13

Szczeklik A, Musial J, Dyczek A, Bartosik A, Milewski M (1995) Autoimmune vasculitis preceding aspirin-induced asthma. Int Arch Allergy Immunol 106:92–94

Szczeklik A, Musial J, Pulka G (1997) Autoimmune vasculitis and aortic stenosis in aspirin-induced asthma (AIA). Allergy 52:352–354

Takaoka A, Tanaka Y, Tsuji T, Jinushi T, Hoshino A, Asakura Y, Mita Y, Watanabe K, Nakaike S, Togashi Y, Koda T, Matsushima K, Nishimura T (2001) A critical role for mouse CXC chemokine(s) in pulmonary neutrophilia during Th type 1-dependent airway inflammation. J Immunol 167:2349–2353

Umetsu DT, McIntire JJ, Akbari O, Macaubas C, DeKruyff RH (2002) Asthma: an epidemic of dysregulated immunity. Nat Immunol 3:715–720

Woolcock AJ, Peat JK (1997) Evidence for the increase in asthma worldwide. Ciba Found Symp 206:122–134 (Discussion 134–129, 157–129)

Ylikoski E, Kinos R, Sirkkanen N, Pykalainen M, Savolainen J, Laitinen LA, Kere J, Laitinen T, Lahesmaa R (2004) Association study of 15 novel single-nucleotide polymorphisms of the T-bet locus among Finnish asthma families. Clin Exp Allergy 34:1049–1055

Yoshida S, Sakamoto H, Yamawaki Y, Shoji T, Akahori K, Onuma K, Nakagawa H, Hasegawa H, Amayasu H (1998) Effect of acyclovir on bronchoconstriction and urinary leukotriene E4 excretion in aspirin-induced asthma. J Allergy Clin Immunol 102:909–914

Zhang Y, Lefort J, Kearsey V, Lapa e Silva JR, Cookson WO, Vargaftig BB (1999) A genome-wide screen for asthma-associated quantitative trait loci in a mouse model of allergic asthma. Hum Mol Genet 8:601–605

Zhu H, Cong JP, Mamtora G, Gingeras T, Shenk T (1998) Cellular gene expression altered by human cytomegalovirus: global monitoring with oligonucleotide arrays. Proc Natl Acad Sci USA 95:14470–14475

Clin Exp Allergy 2005; 35:679–684 doi:10.1111/j.1365-2222.2005.02216.x

Influence of viral infection on the development of nasal hypersensitivity

Y. Okamoto*, Z. Matsuzaki†, T. Matsuoka†, S. Endo†, H. Yamamoto*, H. Chazono*, S. Horiguchi* and T. Hanazawa*

*Department of Otolaryngology, Graduate School of Medicine, Chiba University, Chiba, Japan and †Department of Otolaryngology, Yamanashi Medical University, Yamanashi, Japan

Summary

Background The underlying relationship between viral infections and allergic diseases of the upper respiratory tract has not been well clarified.

Methods In order to clarify the relationship between viral infection and nasal hypersensitivity, mice were sensitized with ovalbumin (OVA) and then infected intranasally with respiratory syncytial virus (RSV), after which their nasal sensitivity to histamine or antigen was examined.

Results Non-sensitized mice showed transient mild nasal hypersensitivity following nasal administration of histamine after intranasal RSV inoculation. In mice sensitized with OVA, RSV infection significantly exaggerated their nasal hypersensitivity to histamine and OVA. Treatment of these mice with a neurokinin (NK)-1/NK-2 receptor antagonist, but not with anti-IL-5 antibodies, reduced their hypersensitivity. The infiltration of nasal mucosa with eosinophils was temporarily associated with accelerated rate of RSV elimination in these animals.

Conclusion RSV infection induced transient nasal hypersensitivity. Several mechanisms, including impairment of nasal epithelial cells are thought to mediate this effect. In allergen-sensitized mice, RSV inoculation strongly enhanced nasal hypersensitivity.

Keywords histamine, nasal hypersensitivity, RSV

Submitted 15 April 2004; revised 24 September 2004; accepted 23 November 2004

Introduction

Recent epidemiological evidence has suggested that acute respiratory viral infections exacerbate the symptoms of pre-existing reactive airway diseases and is the most important trigger of acute asthmatic attacks [1–4]. Viruses, rather than bacteria, cause most acute respiratory tract infections, and asthma attacks in children are often preceded by viral infection [5–7].

The nasal cavity is often the first target of invading viruses, because it is the point of entry into the respiratory tract. The common cold is the most widespread viral infectious condition and is usually caused by viruses such as rhinoviruses, parainfluenza viruses, influenza viruses, adenoviruses and respiratory syncytial virus (RSV) [8, 9]. However, the relationship between viral infections and allergic diseases in the upper respiratory tract has not been well defined. The results from studies that have examined the influence of atopy on the development of the symptom after viral infections are controversial [10–13]. Bardin et al. [11] observed more severe cold symptoms in atopic subjects than in non-atopic subjects after experimental rhinovirus infection. However, in another study, augmented nasal allergic inflammation induced by antigen provocation before viral inoculation did not result in a worsening of cold symptoms [12]. The effects of the common cold on nasal hypersensitivity or allergic rhinitis have not been clearly established.

Nasal responses to viral infection are thought to differ depending on the viral species. Although rhinoviruses causes little damage to epithelial cells in the respiratory tract, RSV induces marked cytopathic effects [13]. RSV is an RNA virus infection which usually results in common cold symptoms, although progression to lower respiratory tract symptoms, the most common being bronchiolitis, frequently occurs in infants. RSV causes about 60% of the bronchitis cases in children [14, 15]. In prospective studies, as many as 75–90% of infants with a clinical diagnosis of bronchiolitis subsequently developed recurrent episodes of wheezing suggestive of childhood asthma and experienced airway histamine or methacholine hypersensitivity which persisted for several years [16–22].

In the present study, we have shown that RSV infection contributes to the exacerbation of nasal hypersensitivity in an allergic rhinitis mouse model.

Materials and Methods

Animals

Eight-week-old male C57BL/6 mice (Nippon Clea, Shizuoka, Japan) that were raised on ovalbumin (OVA)-free chow were

Correspondence: Yoshitaka Okamoto, Department of Otolaryngology, Graduate School of Medicine, Chiba University, 1-8-1 Inohana, Chuo-ku, Chiba 260-8670, Japan.
E-mail: yoka-chiba@k4.dion.ne.jp

used in this study. Hartley strain guinea-pigs (Nippon Clea) were also used to measure passive cutaneous anaphylaxis (PCA). The use of these laboratory animals was approved by the local Animal Ethics Committee (Yamanashi Medical University) and the experiments were conducted in conformity with the guidelines of the committee.

Experimental infection with respiratory syncytial virus

The long strain of RSV (prototype RSV group A strain) was grown in HEp-2 cells in minimal essential medium (MEM) supplemented with 2% fetal calf serum (FCS), 2 mM L-glutamine and antibiotics. RSV was partially purified by polyethylene glycol precipitation, followed by centrifugation in a 35–65% discontinuous sucrose gradient, as described elsewhere [23]. RSV (1×10^6 plaque-forming units (PFU)) in a volume of 20 μL was administered intranasally to mice. Uninfected Hep-2 cells were processed similarly and used as controls.

Virus assay

Lungs and nasal tissues were collected and homogenized in MEM containing 2% FCS and were stored at −70 °C until they were assayed. RSV was assayed by the plaque method using HEp-2 cells in 24-well microplates. The overlay for the plaque assay consisted of MEM supplemented with 2% FCS, antibiotics and 1% methylcellulose. Plates were incubated for 7 days at 37 °C. After the methylcellulose was removed, the plaques were fixed with 10% formaldehyde and stained with 0.1% crystal violet.

Evaluation of sensitivity to histamine in nasal mucosa

One microlitre of various concentrations of histamine, diluted in phosphate-buffered saline (PBS), was administered into each nostril of the experimental mice. The number of nasal rubbing attacks that occurred during the ensuing 10 min was then counted.

Experimental protocol for sensitization with ovalbumin

Mice were immunized with 10 μg OVA (grade V, Sigma Chemical Co., St Louis, MO, USA) intraperitoneally with alum once a week for 4 weeks. Heat-killed bordetella pertussis (1×10^8 bacterial units) was used as an adjuvant in the first immunization. Five days after the last immunization, the mice were either inoculated with RSV or sham-infected with sonicated non-RSV-infected HEp-2 cells. Two micrograms OVA in 2 μL PBS was administered intranasally for 5 consecutive days after the inoculation. Sensitized mice were divided into the following experimental groups and treated as follows. Group 1 consisted of 30 mice treated with a neutralizing IL-5 antibody or a neurokinin (NK)-1/NK-2 antagonist. A rat neutralizing monoclonal antibody (mAb) directed against mouse IL-5 (PharMingen, San Diego, CA, USA) and a control isotype mouse IgGI mAb (PharMingen) were used. Antibodies were injected intraperitoneally twice a week at a dose of 0.1 mg for 1 week before RSV inoculation, and were administered intranasally for 5 consecutive days after inoculation. Group 2 consisted of 10 OVA-sensitized mice who received 0.04 μg of the NK-1/NK-2 antagonist [24] FK224 (Fujisawa Co Ltd, Osaka, Japan) intranasally for 5 consecutive days after RSV inoculation. On the day following the last nasal administration of OVA, the nasal rubbing attacks were counted for 10 min. The sensitivity of the mice to histamine was examined 24 h later in a similar manner.

Treatment of ovalbumin-sensitized mice with a neutralizing anti-interferon-γ monoclonal antibody or with interferon-γ

OVA-sensitized mice received 0.1 mg of anti-IFN-γ neutralizing mAb (PharMingen) or control mAb intraperitoneally twice a week and then intranasally for 5 consecutive days before nasal provocation with OVA. Other OVA-sensitized mice were administered 1 μg of IFN-γ (PharMingen) intranasally for 5 consecutive days before provocation with OVA.

Detection of ovalbumin-specific immunoglobulin E antibody

OVA-specific IgE antibodies were detected by PCA [25]. Briefly, 100 μL of undiluted and twofold diluted serum samples were injected intradermally into the dorsal skin of shaved guinea-pigs. Three days later, the animals were challenged intravenously with 1 mg OVA together with 1% Evans blue. A blue lesion of a diameter greater than 5 mm, as determined 30 min after the challenge, was considered to be positive. PCA titres were expressed as the reciprocal of the highest dilution giving a positive reaction.

Histological examination

On the 4th day after RSV inoculation the mice were killed by CO_2 overdose. The heads of the mice were detached along the line between the upper and lower jaws, and they were then fixed in formalin and decalcified. The section of the nasal cavity anterior to the eyeball was examined and processed for paraffin sectioning. Tissue sections were stained with PAS and the number of infiltrating eosinophils in the whole nasal septum mucosa of each section was determined.

Fluorescence-activated cell sorting analysis

Nasal mucosal tissue from the above mice was cut into small pieces, which were then teased gently through a nylon mesh using frost glass slides. The disrupted mucosa was then suspended in RPMI-1640 containing 10% FCS, penicillin (100 units/mL) and streptomycin (100 μg/mL). After washing twice with medium, $CD3^+$ T cells were purified in 0.2 mL of RPMI-1640 using magnetic beads (Dynal, Great Neck, NY, USA). Following purification, the medium was supplemented with 10% FCS. 10^6 nasal $CD3^+$ T cells collected from seven RSV-infected OVA-sensitized mice or from non-infected OVA-sensitized mice were stained with fluorescein-conjugated anti-CD4 antibody (PharMingen) and fixed overnight with 4% paraformaldehyde (Sigma Chemical Co). The fixed cells were permeabilized by incubation in PBS with 1% bovine serum albumin and 2% saponin (Sigma Chemical Co) for 10 min. A phycoerythrin-conjugated anti-IFN-γ antibody (PharMingen) or an anti-IL-5 antibody (PharMingen), diluted to 20 μg/mL in PBS, was then added. After a 30 min incubation, the cells were washed with PBS and were

analyzed using a FACScan (Becton Dickinson, Fullerton, CA, USA).

Statistical analysis

Comparisons between groups were evaluated using Student's *t* test and Wilcoxon's test.

Results

Viral replication and nasal histamine sensitivity

After nasal inoculation with 10^6 PFU of RSV, mild replication of RSV in the respiratory tract was observed with peak levels occurring in the lung on day 4 and the levels then declined until day 7 as shown previously [26]. RSV was recovered from the nasal mucosa for 12 days after inoculation.

Non-specific stimulation of the nasal mucosa of mice also resulted in nasal rubbings. The number of nasal rubbing attacks observed in 20 normal mice following nasal installation of 2 μL PBS was 9.4 ± 2.9 (mean ± SD). Thus, the lowest histamine concentration administered intranasally in a volume of 2 μL that was needed to induce more than 20 nasal rubbing attacks was defined as the threshold level of nasal histamine hypersensitivity. After RSV inoculation, the threshold decreased and reached its lowest on day 4. It returned to normal by day 14 (Fig. 1(a)).

Influence of respiratory syncytial virus infection on ovalbumin-sensitized mice

The threshold of nasal hypersensitivity to histamine decreased in OVA-sensitized mice and RSV infection in OVA-sensitized mice induced a dramatic enhancement of nasal sensitivity to histamine (Fig. 1(b)). The threshold of nasal hypersensitivity to histamine observed in RSV-infected mice increased gradually after the last nasal administration of OVA and 14 days later, it was the same as that of non-infected mice (data not shown). Fluorescence-activated cell sorting analysis of nasal mucosal T lymphocytes in the RSV-infected OVA-sensitized mice not only revealed an increased expression of IFN-γ, but also of IL-5 (Table 1). Anti-IL-5 treatment of RSV-infected OVA-sensitized mice using neutralizing antibodies reduced the histamine sensitivity in some degree ($P<0.05$) and the treatment with an NK-1/NK-2 antagonist resulted in a marked reduction ($P<0.001$) of the sensitivity (Fig. 1(b)).

After OVA nasal provocation the frequency of nasal rubbing attacks dramatically increased in RSV-infected OVA-sensitized mice, compared with non-infected sensitized mice (Fig. 2). However, anti-IL-5 treatment of RSV-infected OVA-sensitized mice did not significantly improve nasal symptoms after OVA administration. On the other hand, an NK-1/NK-2 antagonist resulted in a significant improvement (Fig. 2).

The number of eosinophils in the nasal mucosa was markedly increased in RSV-infected OVA-sensitized mice compared with those in non-infected OVA-sensitized mice (Fig. 3). The PCA titre, on the other hand, was not significantly different between the two groups (mean ± SD; 21.1 ± 21.0 in infected sensitized mice, 16.6 ± 11.4 in non-infected sensitized mice). Anti-IL-5 treatment of RSV-infected OVA-sensitized mice significantly reduced the number of infiltrated eosinophils, however, the treatment with an NK-1/NK-2 antagonist had no effect on eosinophil infiltration.

The nasal administration of IFN-γ to OVA-sensitized mice increased the number of nasal eosinophils, but had no effect on nasal symptoms (Fig. 4). Treatment with anti-IFN-γ neutralizing antibodies did not affect nasal symptoms or eosinophil infiltration (Fig. 4).

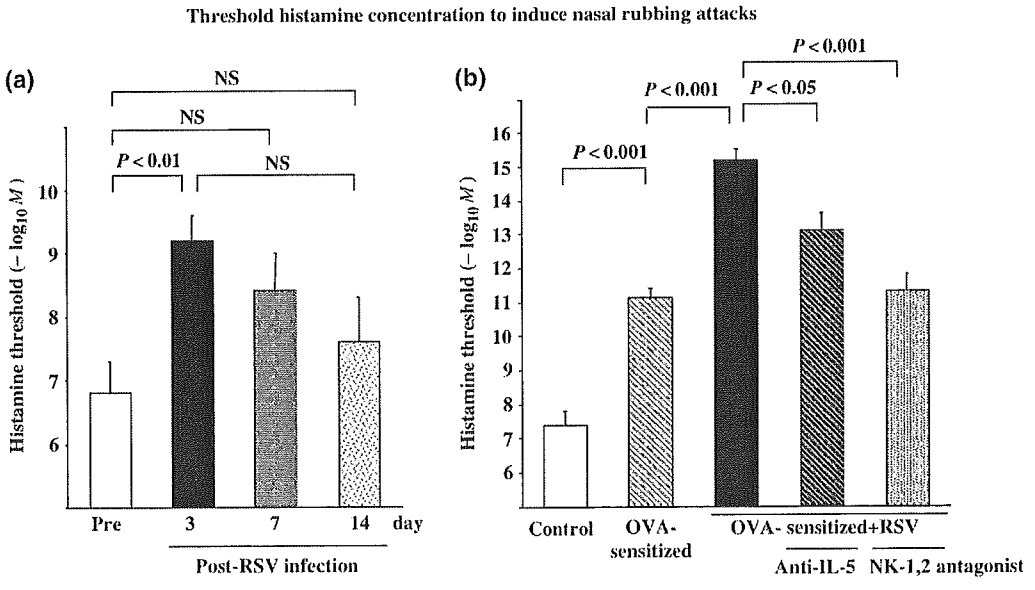

Fig. 1. Threshold histamine concentration needed to induce nasal rubbing attacks in respiratory syncytial virus (RSV)-infected non-sensitized mice (a) and in ovalbumin (OVA)-sensitized mice (b). After RSV inoculation, the threshold decreased transiently and reached its lowest on day 4. Although the threshold decreased in OVA-sensitized mice, RSV infection in OVA-sensitized mice induced a dramatic reduction of the threshold. The treatment with neurokinin (NK)-1/NK-2 receptor antagonist but not with anti-IL-5 neutralizing antibodies improved the reduction. Non-OVA-sensitized mice were used as controls.

Table 1. IL-5 and IFN-γ expression of nasal mucosal T lymphocytes from OVA-sensitized mice*

	RSV-infected mice (%)	Sham-infected mice (%)
IL-5	11.9	6.2
IFN-γ	17.4	11.4

OVA, ovalbumin; RSV, respiratory syncytial virus.
*Mean of two groups and each group consisted of T lymphocytes collected from nasal mucosa of seven mice.

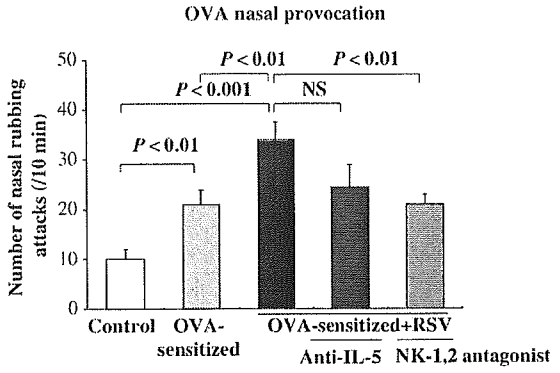

Fig. 2. The number of nasal rubbing attacks in ovalbumin (OVA)-sensitized mice following OVA provocation. Respiratory syncytial virus (RSV) infection in OVA-sensitized mice induced a dramatic enhancement of number of attacks. The anti-IL-5 treatment reduced the enhancement in some degree and the topical administration of the neurokinin (NK)-1/NK-2 receptor antagonist did more.

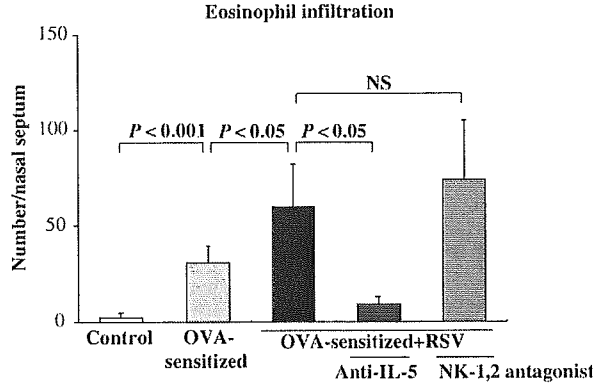

Fig. 3. The number of eosinophils in the nasal mucosa. Respiratory syncytial virus (RSV) infection markedly increased the eosinophil infiltration in ovalbumin (OVA)-sensitized mice. The treatment with anti-IL-5 antibodies reduced the number significantly but not with neurokinin (NK)-1/NK-2 receptor antagonists.

RSV replication on day 4 was significantly reduced in OVA-sensitized mice. However, the use of anti-IL-5 did not exhibit any influence on viral replication and no reduction in viral shedding was observed in anti-IL-5-treated OVA-sensitized mice (Fig. 5).

Discussion

The above studies were designed to examine the mechanism of nasal hypersensitivity observed during viral infections. A murine RSV infection model was used in which the quantitative analysis of nasal rubbing attacks was evaluated as a measure of nasal hypersensitivity. Sneezes in mice are not clearly distinguishable as in humans and are difficult to quantify precisely. The evaluation of nasal obstruction is also difficult, because mice cannot survive by breathing orally. BALB/c mice are known to be sensitive to allergic reactions [27], particularly in the lower respiratory tract, although their nasal reactivity to histamine and other antigens is quite low (data not shown). While C57BL/6 mice are known to mount a Th1 dominant immune response [28], IgE production is inducible in these animals if the correct adjuvant, such as alum, is used, and nasal hypersensitivity can be observed after the topical administration of histamine or antigens. In light of the above and because RSV replication in the nose of BALB/c mice is tolerated well by these animals, we chose to use C57BL/6 mice in our study.

The observations summarized in this report suggest that experimentally induced infection with RSV results in significant enhancement of nasal sensitivity to OVA and histamine in previously sensitized animals. OVA-sensitized animals also exhibited increased expression of IL-5 and IFN-γ and pronounced accumulation of eosinophils in the nasal mucosa after RSV infection.

The mechanisms underlying the development of hypersensitivity states after viral infections such as RSV have not been clinically defined. It is possible that viral infection-associated mucosal damage; recruitment of mast cells, eosinophils and other cellular mediators of hypersensitivity; and activation of cholenergic, adrenergic or non-adrenergic non-cholinergic neurogenic mechanisms may play an important role in the development of mucosal hypersensitivity states [29–31].

In the present studies, pre-treatment with anti-IL-5 resulted in significant decrease in the accumulation of eosinophils. However, such treatment did not influence the degree of viral induced hypersensitivity. In fact, anti-IL-5 treatment was associated with decreased viral elimination in the nasal cavity, and as a result eosinophils may be associated with accelerated RSV elimination. It has been shown that eosinophil cationic protein and eosinophil-derived neurotoxin may act as rebonuclease-dependent antiviral agents [32]. In the present studies, it is interesting to note that use of IFN-γ was associated with increasing eosinophil counts but did not influence nasal hypersensitivity reactions. Thus, although eosinophils may play an important role in viral induced allergic inflammation [33, 34], eosinophils did not seem to contribute to nasal hypersensitivity to OVA in the current experimental setting. IFN-γ is a classical Th1 cytokine that has been shown to reduce allergic reactions when administered during sensitization [35]. However, treatment of OVA-sensitized animals with anti-IFN-γ neutralizing antibody did not decrease nasal sensitivity to OVA during RSV infection.

The observation of particular interest in the current studies is the significant reduction of nasal hypersensitivity detected after the use of NK-1/NK-2 antagonists, although such treatment did not influence eosinophil counts. Recently, it has been shown that infection with RSV frequently is associated with activation of NK receptor sites [36–38]. Tachykinin family of neuropeptides such as substance P have been shown to exhibit strong blinding affinity for NK receptors especially NK-1. Such receptor-neuropeptide interactions are associated

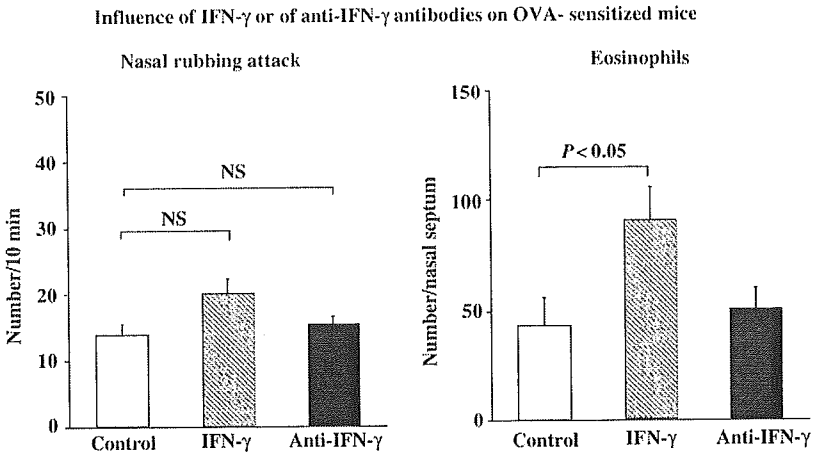

Fig. 4. Influence of IFN-γ and anti-IFN-γ antibodies on ovalbumin (OVA)-sensitized mice. The nasal administration of IFN-γ increased the number of eosinophils, but did not affect the nasal symptoms. Anti-IFN-γ treatment had no effect on either nasal symptoms or eosinophil numbers.

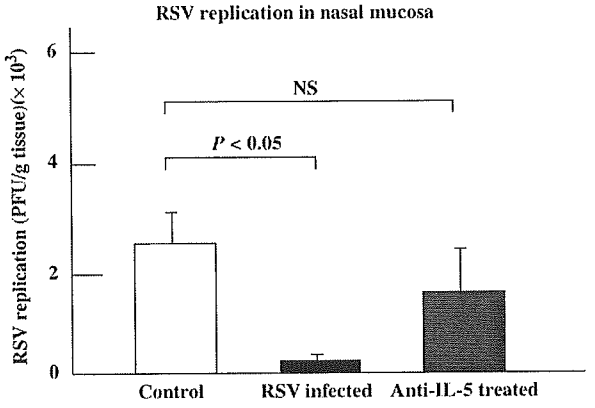

Fig. 5. Respiratory syncytial virus (RSV) replication in the nasal mucosa on day 4 after RSV inoculation. Replication was reduced in ovalbumin (OVA)-sensitized mice, but this reduction was abolished in anti-IL-5-treated OVA-sensitized mice. Non-OVA-sensitized mice were used as controls.

with a wide variety of biologic inflammatory effects, including changes in vascular permeability, mucous secretion, leucocyte chemotaxis and bronchoconstriction [39–41]. It is thus suggested that RSV-associated increase in allergic nasal hypersensitivity to OVA and possibly to other allergens may in part be related to activation of neuropeptide receptors during acute viral infection of the nasal mucosa.

It is possible that increased eosinophil recruitment is mediated by chemokines induced by IFN-γ. Recently induction of eotaxin 3 and IP-10 by IFN-γ in mucosal cell cultures has been demonstrated after experimental RSV infection in *in vivo* settings [42–44]. Based on these reports and the present studies, it is proposed that a possible relationship exists between IFN-γ and induction, recruitment and/or activation of eosinophils in allergic sensitization in the nasal mucosa during viral infections.

Acknowledgements

This work was supported by a Grant-in-Aid for Scientific Research from the Ministry of Education, Science and Culture, Japan. The authors thank Professor Peary L. Ogra for helpful comments

References

1 Green RM, Custovic A, Sanderson G, Hunter J, Johnston SL, Woodcock A. Synergism between allergens and viruses and risk of hospital admission with asthma: case-control study. BMJ 2002; 324:1–5.
2 Message SD, Johnston SL. Viruses in asthma. Br Med Bull 2002; 61:29–43.
3 Gern JE. Viral and bacterial infections in the development and progression of asthma. J Allergy Clin Immunol 2000; 105: s497–502.
4 Johnston SL, Plattemore PK, Sanderson G et al. The relationship between upper respiratory infections and hospital admissions for asthma: a time-trend analysis. Am J Respir Crit Care Med 1996; 154:654–60.
5 Tuffaha A, Gern JE, Lemanske Jr RF. The role of respiratory viruses in acute and chronic asthma. Clin Chest Med 2000; 21:289–300.
6 Schwarze J, Gelfand EW. The role of viruses in development or exacerbation of atopic asthma. Clin Chest Med 2000; 21:279–87.
7 Johnston SL, Pattemore PK, Sanderson G et al. Community study of role of viral infections in exacerbations of asthma in 9–11 year old children. BMJ 1995; 310:1225–9.
8 Makela MJ, Puhakka T, Ruuskanen O et al. Viruses and bacteria in the ethiology of the common cold. J Clin Microbiol 1998; 36:539–42.
9 Irwin RS, Madison JM. The diagnosis and treatment of cough. N Engl J Med 2000; 343:1715–21.
10 Doyle WJ, Skoner DP, Fireman P et al. Rhinovirus 39 infection in allergic and non-allergic subjects. J Allergy Clin Immunol 1992; 89:968–78.
11 Bardin PG, Fraenkel DJ, Sanderson G et al. Amplified rhinovirus colds in atopic subjects. Clin Exp Allergy 1994; 24:457–64.
12 Avila PC, Abisheganaden JA, Wong H et al. Effects of allergic inflammation of the nasal mucosa on the severity of rhinovirus 16 cold. J Allergy Clin Immunol 2000; 105:923–32.
13 Folkerts G, Busse WW, Nikamp FP, Sorkness R, Gern JE. Virus-induced airway hyperresponsiveness and asthma. Am J Respir Crit Care Med 1998; 157:1708–720.

14 Van Schaik SM, Welliver RC, Kimpen JK. Novel pathways in the pathogenesis of respiratory syncytial virus disease. Pediatr Pulmonol 2000; 30:131–8.
15 Shay DK, Holman RC, Newman RD, Liu LL, Stout JW, Anderson LJ. Bronchiolitis-associated hospitalizations among US children, 1980–1999. JAMA 1999; 282:1440–6.
16 Sigurs N, Bjarnason R, Sigurbergsson F, Kjellman B. Respiratory syncytial virus bronchiolitis in infancy is an important risk factor for asthma and allergy at age 7. Am J Respir Crit Care Med 2000; 161:1501–7.
17 Sigurs N, Bjarnason R, Sigurbergsson F, Kjellman B, Bjorksten B. Asthma and immunoglobulin E antibodies after respiratory syncytial virus bronchiolitis: a prospective cohort study with matched controls. Pediatrics 1995; 95:500–5.
18 Hall CB, Hall WJ, Gala CL, MaGill FB, Leddy JP. Long-term prospective study in childrem after respiratory syncytial virus infection. J Pediatr 1984; 105:358–64.
19 Eisen AH, Bacal HL. The relationship of acute bronchiolitis to bronchial asthma-a 4 to 14-year follow up. Pediatrics 1963; 31: 859–61.
20 Sims DG, Downham MAPS, Gardner PS, Webb JKG, Weighman D. Study of 8-year-old children with a history of respiratory syncytial virus bronchiolitis in infancy. BMJ 1978; 1:11–4.
21 Welliver RC, Duffy L. The relationship of RSV-specific immunoglobulin E antibody responses in infancy, recurrent wheezing, and pulmonary function at age 7–8 years. Pediatr Pulmonol 1993; 15:19–27.
22 Pullan CR, Hey EM. Wheezing, asthma, and pulmonary dysfunction 10 years after infection with respiratory syncytial virus in infancy. Br Med J 1982; 284:1665–9.
23 Ueba O. Respiratory syncytial virus 1 concentration and purification of the infectious virus. Acta Med Okayama 1978; 32:265–72.
24 Morimoto H, Murai M, Maeda Y et al. FK224, a novel cyclopeptide substance P antagonist with NK1 and NK2 receptor selectivity. J Pharmacol Exp Ther 1992; 262:398–402.
25 Mota I, Wong D. Homologous and heterologous passive cutaneous anaphylactic activity of mouse antisea during the course of immunization. Life Sci 1969; 8:813–20.
26 Matsuoka T, Okamoto Y, Matsuzaki Z et al. Characteristics of immunity induced by viral antigen or conferred by antibody via different administration routes. Clin Exp Immunol 2002; 130: 386–92.
27 Sato M, Iwakabe K, Ohta A, Sekimoto M, Kimura S, Nishimura T. Self-priming cell culture system for monitoring genetically controlled spontaneous cytokine-producing ability in mice. Immunol Lett 1999; 70:173–8.
28 Shankar AH, Titus RG. T cell and non-T cell compartments can independently determine resistance to Leishmania major. J Exp Med 1995; 181:845–55.
29 Fryer AD, Jacoby DB. Parainfluenza virus infection damages inhibitory M_2 muscarinic receptors on pulmonary parasympathetic nerves in the guinea-pig. Br J Pharmacol 1991; 102:267–71.
30 Jacoby DB, Fryer AD. Interaction of viral infections with muscarinic receptors. Clin Exp Allergy 1999; 29: 59–64.
31 Adamko DJ, Yost BL, Gleich GJ, Fryer AD, Jacoby DB. Ovalbumin sensitization changes the inflammatory responses to subsequent parainfluenza infection: eosinophils mediate airway hyperresponsiveness, M_2 muscarinic receptor dysfunction, and antiviral effects. J Exp Med 1999; 190:1465–77.
32 Domachowske JB, Dyer KD, Adams AG, Leto TL, Rosenberg HF. Eosinophil cationic protein1 R Nase 3 is anather RNase A-family ribonuclease with direct antivial activity. Nucleic Acids Res 1998; 26:5327–32.
33 Kay AB. Modulation of eosinophil function in vitro. Clin Exp Allergy 1990; 20:31–4.
34 Terada N, Konno A, Tada H, Shirotori K, Ishikawa K, Togawa K. The effect of recombinant human interleukin-5 on eosinophil accumulation and degranulation in human nasal mucosa. J Allergy Clin Immunol 1992; 90:160–8.
35 Young HA, Hardy KJ. Role of interferon-gamma in immune cell regulation. J Leukocyte Biol 1995; 58:373–81.
36 Piedimonte G, Rodriguez MM, King KA, McLean S, Jiang X. Respiratory syncytial virus upregulates expression of the substance P receptor in rat lung. Am J Physiol 1999; 277:L831–40.
37 King KA, Hu C, Rodriguez MM, Jiang X, Piedimonte G. Exaggerated neurogenic inflammation and substance P receptor upregulation in RSV-infected weanling rate. Am J Respir Cell Mol Biol 2001; 24:101–7.
38 Tripp RA, Barskey A, Goss L, Anderson LJ. Substance P receptor expression on lymphocytes is associated with the immune response to respiratory syncytial virus infection. J Neuroimmunol 2002; 129:141–53.
39 Konno A, Numata T, Terada N, Hanazawa T, Nagata H, Motosugi H. Role of substance P in the vascular response of nasal mucosa in nasal allergy. Ann Otol Rhinol Laryngol 1996; 105:648–53.
40 Gungor A, Baroody FM, Naclerio RM, White SR, Corey JP. Decreased neuropetide release may play a role in the pathogenesis of nasal polyps. Otolaryngol Head Neck Surg 1999; 121: 585–90.
41 Okamoto Y, Shirotori K, Kudo K et al. Cytokine expression after the topical administration of substance P to human nasal mucosa. J Immunol 1993; 151:4391–8.
42 Yamamoto S, Kobayashi I, Tsuji K et al. Upregulation of IL-4R by IFN-γ: enhanced IL-4 induced eotaxin-3 production in airway epithelium. Am J Respir Cell Mol Biol 2004.
43 Azuma MA, Szczepanik M, Tsuji RF et al. Early delaved-type hypersensitivity eosinophil infiltrares depend on T helper 2 cytokines and interferon-γ via CXCR3 chemokines. Immunology 2004; 111:306–17.
44 Li H, Chunsong H, Guobin C et al. Highly up-regulated CXCR2 expression on eosinophils in mice infected with *Schistosoma japonicum*. Immunology 2004; 111:107–17.

IMAGES IN CLINICAL MEDICINE

Airway Dilatation after Inhalation of a Beta-Agonist

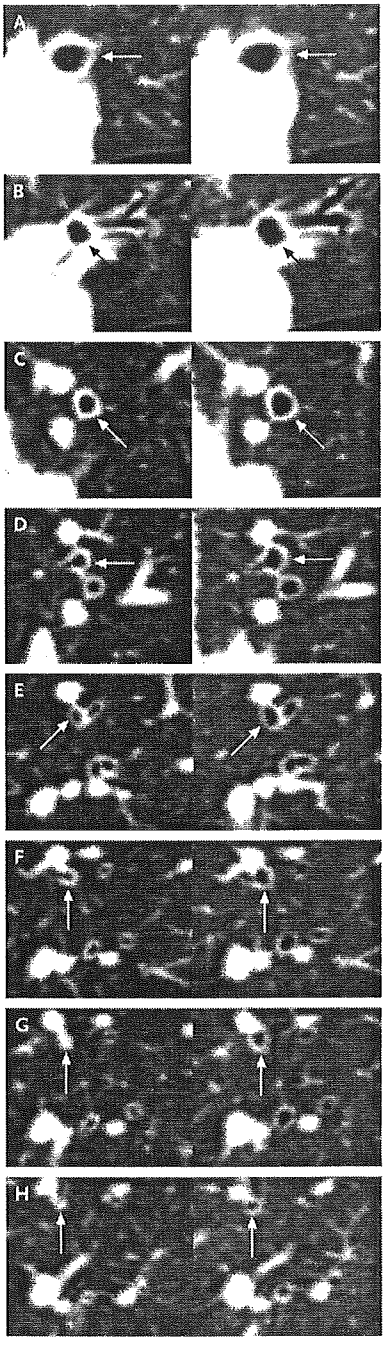

A 37-YEAR-OLD WOMAN WITH A 25-YEAR HISTORY OF ASTHma that had been managed with inhaled budesonide and albuterol (salbutamol) as needed underwent high-resolution multislice helical computed tomographic scanning. Thirty minutes after the inhalation of albuterol, a cross-sectional multiplanar reconstruction of the right upper lobe, obtained at maximal inspiration, revealed an increase in the airway caliber. Each panel of images from these two videos consists of the view before the inhalation on the left and the corresponding view after the inhalation on the right. Panel A shows the segmental, or third-generation, bronchus (arrows); Panel B the fourth-generation bronchus at the branching point (arrows); and Panel C more of the periphery of the fourth-generation bronchus, with full wall visualization (arrows). Panels D, E, F, and G show bronchial divisions from the fifth to the eighth generation (arrows); the same bronchial divisions are shown in the video clip. Panel H shows preinhalation airway occlusions (left-hand image), which opened up after the inhalation (right-hand image). The forced expiratory volume in one second, initially 1.27 liters (49.8 percent of the predicted value), increased by 0.49 liter after the inhalation of albuterol. It is important to note that airway resistance is an inverse function of the airway radius to the fourth to fifth power.

Gen Tamura, M.D.

Tohoku University Hospital
Sendai 980-8574, Japan

Yuji Suda, M.D.

Sendai City Medical Center
Sendai 983-0824, Japan

Involvement of TNF Receptor-Associated Factor 6 in IL-25 Receptor Signaling[1]

Yuko Maezawa,* Hiroshi Nakajima,[2]* Kotaro Suzuki,* Tomohiro Tamachi,* Kei Ikeda,* Jun-ichiro Inoue,† Yasushi Saito,* and Itsuo Iwamoto*

IL-25 (IL-17E) induces IL-4, IL-5, and IL-13 production from an unidentified non-T/non-B cell population and subsequently induces Th2-type immune responses such as IgE production and eosinophilic airway inflammation. IL-25R is a single transmembrane protein with homology to IL-17R, but the IL-25R signaling pathways have not been fully understood. In this study, we investigated the signaling pathway under IL-25R, especially the possible involvement of TNFR-associated factor (TRAF)6 in this pathway. We found that IL-25R cross-linking induced NF-κB activation as well as ERK, JNK, and p38 activation. We also found that IL-25R-mediated NF-κB activation was inhibited by the expression of dominant negative TRAF6 but not of dominant negative TRAF2. Furthermore, IL-25R-mediated NF-κB activation, but not MAPK activation, was diminished in TRAF6-deficient murine embryonic fibroblast. In addition, coimmunoprecipitation assay revealed that TRAF6, but not TRAF2, associated with IL-25R even in the absence of ligand binding. Finally, we found that IL-25R-mediated gene expression of IL-6, TGF-β, G-CSF, and thymus and activation-regulated chemokine was diminished in TRAF6-deficient murine embryonic fibroblast. Taken together, these results indicate that TRAF6 plays a critical role in IL-25R-mediated NF-κB activation and gene expression. *The Journal of Immunology,* **2006, 176: 1013–1018.**

Interleukin-25 has recently been identified as the fifth member of the IL-17 cytokine family (IL-17E) by database searching (1–4). The IL-17 family now consists of six family members, namely IL-17 (IL-17A), IL-17B, IL-17C, IL-17D, IL-25, and IL-17F (5–7). Among IL-17 family members, IL-25 is less homologic to other IL-17 family members, e.g., 18% homology to IL-17A at amino acid level. Accordingly, in vivo biologic activities of IL-25 are markedly different from those described for IL-17 and other IL-17 family cytokines (2–4, 8–10). Remarkably, it has been shown that the enforced expression of IL-25 induces IL-4, IL-5, and IL-13 production from an unidentified non-T/non-B cell population and subsequently induces Th2-type immune responses such as eosinophilic airway inflammation, mucus production, and airway hyperreactivity (2–4, 8).

IL-25R, which is also called IL-17BR, IL-17Rh1, or Evi27, is a 56-kDa single transmembrane protein with homology to IL-17R (1, 11, 12). IL-25R was first identified as a receptor for IL-17B (11) but IL-25R has subsequently been shown to exhibit a higher affinity for IL-25 than for IL-17B (1). IL-25 has also been demonstrated to activate NF-κB and induce IL-8 production in a human renal carcinoma cell line (1). However, the molecular components consisting of IL-25R signaling pathways and their regulation are still largely unknown.

It has recently been shown that TNFR-associated factor (TRAF)[3] family proteins play a critical role in a number of signaling pathways that activate NF-κB (13–16). TRAF family proteins contain a conserved TRAF-C domain that is essential for the interaction with their cognate receptors or cytoplasmic signaling proteins (13–16). Among TRAF family proteins, TRAF6 exhibits the unique properties in that its TRAF-C domain interacts with a peptide motif distinct from that recognized by other TRAF proteins (17), supporting the findings that TRAF6 exhibits various functions in regulating adaptive and innate immunity, bone metabolism, and cell apoptosis (13–16). The structural analysis of the peptide-TRAF6 interaction has clarified the TRAF6-binding motif as X-X-Pro-X-Glu-X-X-(aromatic/acidic residue) (17). The TRAF6-binding motif is found not only in adaptor proteins such as IL-1R-associated kinase (17) and TIFA (18) but also in membrane-bound proteins such as CD40 and the receptor activator of NF-κB RANK (17). Importantly, the TRAF6-binding motif is present in human and murine IL-25R.

In the present study, we investigated whether TRAF6 is involved in IL-25R signaling. Our results have clearly demonstrated a critical involvement of TRAF6 in IL-25R-mediated NF-κB activation and gene expression.

Materials and Methods

Cell culture

X63 cells were maintained in RPMI 1640 medium with 10% FCS, 50 μM 2-ME, and antibiotics (complete RPMI 1640 medium). Ba/F3 cells were cultured in complete RPMI 1640 medium supplemented with 10% (v/v) of the supernatant of murine IL-3-producing X63 cells (X63-IL-3; a gift from Dr. H. Karasuyama, Tokyo Medical and Dental University, Tokyo, Japan) (19). COS7 cells were cultured in DMEM supplemented with 10% FCS

*Department of Allergy and Clinical Immunology, Graduate School of Medicine, Chiba University, Chiba, Japan; and †Division of Cellular and Molecular Biology, Department of Cancer Biology, Institute of Medical Science, University of Tokyo, Tokyo, Japan

Received for publication March 2, 2005. Accepted for publication November 2, 2005.

The costs of publication of this article were defrayed in part by the payment of page charges. This article must therefore be hereby marked *advertisement* in accordance with 18 U.S.C. Section 1734 solely to indicate this fact.

[1] This work was supported in part by grants from Special Coordination Funds for Promoting Science and Technology from the Ministry of Education, Culture, Sports, Science and Technology, Japan.

[2] Address correspondence and reprint requests to Dr. Hiroshi Nakajima, Department of Allergy and Clinical Immunology, Graduate School of Medicine, Chiba University, 1-8-1 Inohana, Chiba City, Chiba 260-8670, Japan. E-mail address: nakajimh@faculty.chiba-u.jp

[3] Abbreviations used in this paper: TRAF, TNFR-associated factor; TARC, thymus and activation-regulated chemokine; MEF, murine embryonic fibroblast; DN, dominant negative; MKK, MAPK kinase; WT, wild type.

0022-1767/06/$02.00

and antibiotics (complete DMEM). Wild-type (WT) murine embryonic fibroblast (MEF), TRAF6-deficient (TRAF6$^{-/-}$) MEF (20), and Plat-E cells (21) were established and maintained as described elsewhere.

Plasmids

DNA fragment coding the extracellular domain of murine IL-25R, a gift from Dr. J. D. Shaughnessy (University of Arkansas for Medical Sciences, Little Rock, AR) (12) was fused to the fragment coding C-terminal 187 aa of MPL, a receptor for thrombopoietin (22), and cloned into expression vector pCDNA3 (pCDNA3 IL-25R-MPL). Expression vectors for WT TRAF2, dominant negative (DN) TRAF2, Flag-tagged WT TRAF6, and Flag-tagged DN TRAF6 were previously described (23). Expression vectors for Flag-tagged IL-25 (BCMGS Flag-IL-25), Flag-tagged IL-25R (pCMV1 Flag-IL-25R), and *myc*-tagged intracellular region of IL-25R (pCDNA3 *myc*-IL-25R) were constructed by PCR amplification using PFU polymerase (Stratagene). The DNA fragment coding Flag-tagged IL-25R was subsequently subcloned into the retrovirus vector pMX IRES-GFP to generate pMX Flag-IL-25R-IRES-GFP. Alanine substitution of IL-25R on glutaminic acid at aa 338 (IL-25R E338A) was generated by using a PCR-based site-directed mutagenesis kit (Stratagene). The mutation was confirmed by DNA sequencing.

Cytokines

X63 cells were transfected with BCMGS Flag-IL-25 to generate murine IL-25-producing X63 cells (X63-IL-25). The supernatant of X63-IL-25 cells was collected and used as a source of IL-25. The supernatant of murine IL-3-producing X63 cells (X63-IL-3) and the empty vector (BCMGS neo)-transfected X63 cells (X63-control) were also used as controls.

Bioassay for IL-25

IL-3-dependent Ba/F3 cells were transfected with pCDNA3 IL-25R-MPL and Ba/F3 cells that stably expressed IL-25R-MPL were selected by G418 (Ba/F3 IL-25R-MPL cells). The expression of IL-25R-MPL was evaluated not only at mRNA levels by RT-PCR analysis but also at protein levels with the response to the supernatant of X63-IL-25 cells. Subsequently, bioactivity of IL-25 was assessed by the proliferative response of Ba/F3 IL-25R-MPL cells. Briefly, Ba/F3 IL-25R-MPL cells (2×10^3 cells/well) were cultured in triplicate at 37°C in 96-well plates in the complete RPMI 1640 medium in the presence of X63-IL-25 conditioned medium or X63-IL-3 conditioned medium (as a positive control) for 36 h with 0.5 μCi of [^{3}H]thymidine added for the final 12 h. Empty vector (pCDNA3)-transfected Ba/F3 cells were used as a negative control.

Retrovirus-mediated expression of IL-25R in MEF

A transient retrovirus packaging cell line of Plat-E cells (2×10^6) was transfected with 3 μg of pMX Flag-IL-25R-IRES-GFP using FuGENE6 transfection reagents (Roche Diagnostics). At 24 h after the transfection, the medium was once changed and another 24 h later, the supernatant was harvested as virus stocks and stored at −80°C until use. WT MEF or TRAF6$^{-/-}$ MEF (1×10^6) were infected with 2 ml of virus stocks for 4 h in the presence of polybrene (1 μg/ml) and then diluted and maintained in the complete DMEM. Under these conditions, the efficiency of infection was 90% as assessed by GFP$^+$ cells by FACS.

Luciferase assay

COS7 cells (1×10^5) were transfected with 1.0 μg of pCMV1 Flag-IL-25R and 0.3 μg of NF-κB-responding *Photinus pyralis* luciferase reporter vector pNF-κB-Luc (Stratagene) using FuGENE6. In some experiments, expression vector for DN TRAF6 or DN TRAF2 was cotransfected. Empty vector was added to adjust the total amount of plasmid DNA for transfection. To normalize for transfection efficiency, 10 ng of *Renilla reniformis* luciferase reporter vector pRL-TK was added to each transfection. At 24 h after the transfection, cells were stimulated with X63-IL-25 condition medium or anti-Flag M2 mouse mAb (2 μg/ml; Sigma-Aldrich) at 37°C for 24 h, and the luciferase activity of *Photinus pyralis* and *Renilla reniformis* were determined by the Dual-Luciferase Reporter Assay System (Promega). *Photinus pyralis* luciferase activity of pNF-κB-Luc was normalized by *Renilla reniformis* luciferase activity of pRL-TK. Condition medium of X63-control cells or mouse monoclonal IgG1 (Ancell) was used as controls.

Nuclear accumulation of NF-κB p65

WT MEF or TRAF6$^{-/-}$ MEF were infected with retrovirus of pMX Flag-IL-25R-IRES-GFP as described earlier and Flag-IL-25R-expressing WT MEF or TRAF6$^{-/-}$ MEF were stimulated with X63-IL-25 condition medium or anti-Flag M2 mAb (2 μg/ml) at 37°C for 30 min. Nuclear extracts were prepared as described elsewhere (24), and DNA-binding activity of NF-κB p65 in the nuclear extracts was detected by Transfactor NF-κB chemiluminescent kit (BD Biosciences) according to the manufacturer's instruction. Briefly, nuclear extracts (5 μg) were added to wells coated with NF-κB consensus oligonucleotides and incubated for 1 h at room temperature. After washing, the wells were incubated with anti-NF-κB p65 rabbit polyclonal Ab, followed by anti-rabbit IgG HRP and then chemiluminescent substrate mixture. Chemiluminescent intensities were measured with Arvo 1420 multilabel counter (Wallac). For DNA competition experiments, 0.5 μg of unlabeled competitor oligonucleotide was added to the nuclear extracts.

Immunoblotting

MEF (1×10^5) were starved from FCS for over 12 h and then stimulated with anti-Flag mAb (2 μg/ml), mouse rIL-17 (100 ng/ml; R&D Systems), or mouse rIL-1β (10 ng/ml; PeproTech) for 30 min. The cells were then lysed with cell lysis buffer (10 mM Tris-HCl, 150 mM NaCl, 2 mM EDTA, 0.875% Brij97, 0.125% Nonidet P-40, 8 mM DTT, and 1% protease inhibitor mixture (Sigma-Aldrich)) supplemented with 1 mM Na_3VO_4, 10 mM NaF, and 60 mM β-glycerophosphate. The aliquot of lysates was applied for SDS-PAGE. The following Abs were used for immunoblotting: anti-IκB-α (MBL Japan), anti-p38α/SAP2a, anti-p38 (pT180/pY182), anti-ERK1, anti-ERK1/2 (pT202/pT204), anti-pan JNK/SAPK1, and anti-JNK (pT183/pT185) (BD Transduction).

Coimmunoprecipitation assay

COS7 cells (4×10^5) were transfected with pCDNA3 *myc*-IL-25R (1.0 μg) and/or pME18S Flag-TRAF6 (1.0 μg), pME18S Flag-TRAF2 (1.0 μg), or pME18S Flag-TRAF5 (1.0 μg) using FuGENE6. Twenty-four hours after the transfection, cells were harvested, lysed with cell lysis buffer, and centrifuged to remove cellular debris. After preclearation, the supernatants were immunoprecipitated with either anti-*myc* mAb (9E10; Santa Cruz Biotechnology) or anti-Flag M2 mAb and 100 μl of protein G-Sepharose (Pharmacia). The immunoprecipitates or the aliquot of whole cell lysates were applied for immunoblotting with rabbit polyclonal anti-Flag Ab (Sigma-Aldrich) or biotin-labeled anti-*myc* mAb (9E10; Santa Cruz Biotechnology).

RT-PCR

Total cellular RNA was prepared, and RT-PCR analysis was performed as previously described (24). In brief, Flag-IL-25R-expressing WT MEF or TRAF6$^{-/-}$ MEF were stimulated with anti-Flag mAb (2 μg/ml) at 37°C for 3 h and the total cellular RNA was isolated using Isogen solution (Nippon Gene) according to the manufacturer's instruction. The following primer pairs were used for PCR: IL-6 (ATGAAGTTCCTCTCTGCAA GAG and GTTTGCCGAGTAGATCTCAAAG), G-CSF (GCTGTG GCAAAGTGCACTATG and AAGCCCTGCAGGTACGAAATG), TGF-β (ATTCAGCGCTCACTGCTCTTG and TCAGCTGCACTTG CAGGAGC), and thymus and activation-regulated chemokine (TARC) (TGAGGTCACTTCAGATGCTGC and ACCAATCTGATGGCCT TCTTC). RT-PCR for β-actin was performed as a control. All PCR amplifications were performed at least three times with multiple sets of experimental RNAs.

Data analysis

Data are summarized as mean ± SD. The statistical analysis of the results was performed by the unpaired *t* test. Values for $p < 0.05$ were considered significant.

Results

Establishment of a bioassay for IL-25

It has been reported that IL-25 activates NF-κB in a renal carcinoma cell line (1), but the signaling pathway under IL-25R is largely unknown. To examine IL-25 signaling in detail, we first prepared rIL-25 and an assay that verifies the bioactivity of rIL-25. Because IL-25 belongs to the cystine knot family and correct refolding and dimer formation seem to be required for its biological activity (6, 7), we used the mammalian cell-based cytokine expression system (19) rather than the *Escherichia coli*-based expression system. We first established X63 cells that stably produced mouse IL-25 (X63-IL-25 cells) and used the supernatant of

X63-IL-25 cells as a source of IL-25. To evaluate the bioactivity of the produced IL-25, we established Ba/F3 cells that expressed IL-25R-MPL fusion protein (Ba/F3 IL-25R-MPL cells) and used as a responding cell for IL-25 stimulation. As shown in Fig. 1, Ba/F3 IL-25R-MPL cells proliferated in response not only to the supernatant of X63-IL-3 cells but also to the supernatant of X63-IL-25 cells in a dose-dependent manner, whereas control Ba/F3 cells proliferated in response to the supernatant of X63-IL-3 cells but not to the supernatant of X63-IL-25 cells. As expected, either Ba/F3 IL-25R-MPL cells or control Ba/F3 cells did not proliferate in response to the supernatant of X63-control cells (Fig. 1).

IL-25R cross-linking induces NF-κB activation

We next established the system that mimicked IL-25R signaling to clarify the IL-25 signaling pathway in detail. To eliminate the possible involvement of the endogenously expressed IL-25R, we used Ab-mediated cross-linking of the receptors rather than ligand-mediated activation. Either WT IL-25R or Flag-IL-25R was expressed in COS7 cells, and these cells were stimulated with the supernatant of X63-IL-25 cells or anti-Flag mAb. In cells expressing WT IL-25R, the supernatant of X63-IL-25 cells, but not stimulation with anti-Flag mAb, activated the NF-κB-responding reporter construct (Fig. 2*A*). In contrast, in cells expressing Flag-IL-25R, both the supernatant of X63-IL-25 cells and anti-Flag mAb activated NF-κB-responding reporter construct (Fig. 2*A*). These results indicate that IL-25R signaling induces NF-κB activation and that the cross-linking with anti-Flag mAb mimics the ligand-mediated signaling of IL-25 in cells expressing Flag-IL-25R.

TRAF6 is crucial for IL-25R-mediated NF-κB activation

It has been reported that TRAF6 is involved in the signaling pathways of IL-1- and IL-17-induced NF-κB activation (20, 25, 26). To determine whether TRAF6 is involved in IL-25R-mediated signaling, we investigated the effect of a DN TRAF6 on IL-25R-mediated NF-κB activation. As a control, we examined the effect of DN TRAF2 on IL-25R-mediated NF-κB activation in parallel. As shown in Fig. 2*B*, the expression of DN TRAF6, but not DN TRAF2, inhibited IL-25R-mediated NF-κB activation in a dose-dependent manner ($n = 4$, $p < 0.01$), suggesting that TRAF6 but not TRAF2 is involved in the signaling pathways of NF-κB activation under IL-25R.

To further clarify the involvement of TRAF6 in IL-25R-mediated signaling, we compared IL-25R-mediated IκB-α down-regulation in Flag-IL-25R-expressing TRAF6$^{-/-}$ MEF and in Flag-IL-25R-expressing WT MEF. As controls, these cells were stimulated

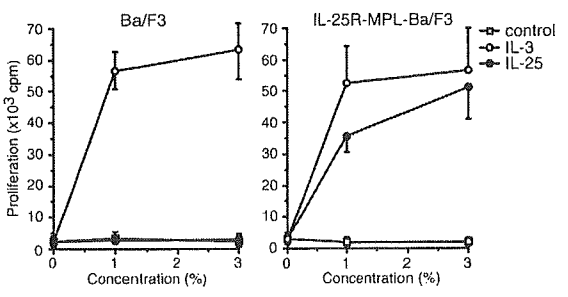

FIGURE 1. Establishment of a bioassay for IL-25. Control vector-transfected Ba/F3 cells (*left*) and IL-25R-MPL-expressing Ba/F3 cells (*right*) were cultured in the presence of the supernatant of X63-control, X63-IL-3, or X63-IL-25 cells at the indicated concentrations at 37°C for 36 h with 0.5 μCi of [^{3}H]thymidine added for the final 12 h. Data are mean ± SD of [^{3}H]thymidine incorporation for four independent experiments.

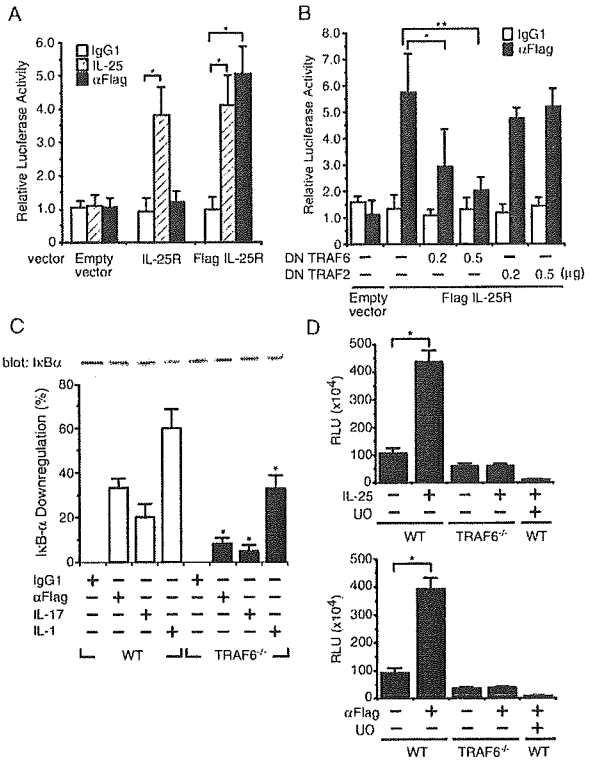

FIGURE 2. IL-25R signaling induces NF-κB activation by a TRAF6-dependent mechanism. *A*, IL-25R cross-linking induces NF-κB activation. COS7 cells were transfected with the expression vector for IL-25R or Flag-tagged-IL-25R in the presence of pNF-κB-Luc and pRL-TK. Twenty-four hours later, the cells were stimulated with the supernatant of X63-IL-25 cells (3%) or anti-Flag mAb (2 μg/ml) at 37°C for 24 h. Luciferase activities of pNF-κB-Luc were determined by a Dual-Luciferase Reporter System. Data are mean ± SD of the relative luciferase activity of pNF-κB-Luc for four experiments. Significantly different (*, $p < 0.01$) from the mean value of unstimulated cells (control IgG1). *B*, DN TRAF6 inhibits IL-25R-mediated NF-κB activation. The expression vector for Flag-tagged IL-25R was transfected to COS7 cells in the presence of pNF-κB-Luc and pRL-TK. Where indicated, amounts of expression vector for DN TRAF6 or DN TRAF2 were simultaneously transfected. Twenty-four hours later, cells were incubated with anti-Flag mAb or control IgG1 at 37°C for another 24 h, and the luciferase activities of pNF-κB-Luc were determined by the Dual-Luciferase Reporter Assay System. Data are mean ± SD for four experiments. Significant difference (*, $p < 0.05$ and **, $p < 0.01$) is shown. *C*, IL-25R-mediated IκB-α down-regulation is diminished in TRAF6$^{-/-}$ cells. WT MEF and TRAF6$^{-/-}$ MEF were infected with retrovirus of pMX-Flag-IL-25R-IRES-GFP as described in *Materials and Methods*. After infected cells were sorted and expanded, IL-25R was cross-linked with anti-Flag mAb or control IgG1 at 37°C for 20 min. As controls, MEF infected with retrovirus of pMX-Flag-IL-25R-IRES-GFP were stimulated with rIL-17 (100 ng/ml) or IL-1β (10 ng/ml) at 37°C for 20 min. Cell lysates were subjected to immunoblotting with anti-IκB-α Ab. Shown are representative blot (*top*) and mean ± SD of the percentage of IκB-α down-regulation determined by a densitometer (*bottom*) from four independent experiments. Significantly different (*, $p < 0.01$) from the mean value of the corresponding response of WT MEF. *D*, TRAF6 is required for IL-25-induced nuclear accumulation of NF-κB p65. Flag-IL-25R-expressing WT MEF or TRAF6$^{-/-}$ MEF were stimulated with X63-IL-25 condition medium (*top*) or anti-Flag mAb (*bottom*) at 37°C for 30 min. As controls, supernatant of X63-control cells (*top*) or control IgG1 (*bottom*) was used. Nuclear extracts were prepared from these cells, and the binding activity to NF-κB consensus oligonucleotides was determined as described in *Materials and Methods*. Where indicated, unlabeled competitor oligonucleotides were added to nuclear extracts to confirm specific binding. Data are mean ± SD of relative light unit (RLU) for four experiments. Significant difference (*, $p < 0.01$) are indicated.

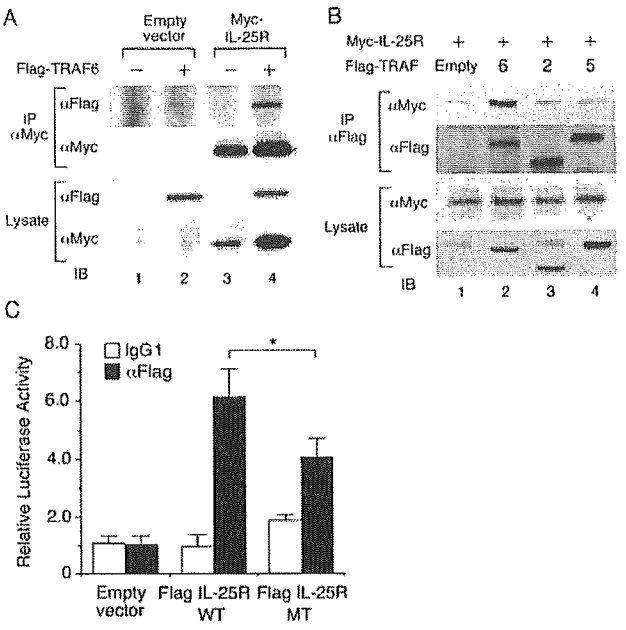

FIGURE 3. TRAF6 but not TRAF2 nor TRAF5 associates with IL-25R. *A*, TRAF6 associates with IL-25R. COS7 cells were transfected with *myc*-tagged IL-25R and/or Flag-tagged TRAF6, and the cell lysates were immunoprecipitated (IP) with anti-*myc* Ab and followed by immunoblottings (IB) with anti-Flag Ab or anti-*myc* Ab. Shown are representative data of three independent experiments. *B*, TRAF2 and TRAF5 do not associate with IL-25R. COS7 cells were transfected with *myc*-tagged IL-25R and Flag-tagged TRAF6, Flag-tagged TRAF2, or Flag-tagged TRAF5. Cell lysates were immunoprecipitated with anti-Flag Ab and followed by immunoblottings with anti-*myc* Ab or anti-Flag Ab. Shown are representative data of three independent experiments. *C*, E338A mutation of IL-25R attenuates IL-25R-mediated NF-κB activation. COS7 cells were transfected with the expression vector for Flag-tagged IL-25R WT or Flag-tagged-IL-25R E338A (Flag IL-25R MT) in the presence of pNF-κB-Luc and pRL-TK. Twenty-four hours later, the cells were stimulated with anti-Flag mAb (2 μg/ml) at 37°C for 24 h. Luciferase activities of pNF-κB-Luc were determined by a Dual-Luciferase Reporter System. Data are means ± SD of the relative luciferase activity of pNF-κB-Luc for four experiments. Significant difference (*, $p < 0.05$) is shown.

with IL-1β or IL-17, cytokines that activate the NF-κB pathway (5–7, 20, 27). As shown in Fig. 2*C*, the expression levels of IκB-α in Flag-IL-25R-expressing WT MEF were down-regulated in response to anti-Flag mAb, compared with the basal levels of IκB-α (control IgG1) ($n = 4$, $p < 0.01$). Stimulation with the supernatant of X63-IL-25 cells also down-regulated the expression levels of IκB-α in Flag-IL-25R-expressing WT MEF (data not shown). Importantly, IL-25R-mediated IκB-α down-regulation was significantly impaired in Flag-IL-25R-expressing TRAF6$^{-/-}$ MEF, compared with that in Flag-IL-25R-expressing WT MEF ($n = 4$, $p < 0.01$) (Fig. 2*C*). As expected, IL-1- or IL-17-mediated IκB-α down-regulation was also impaired in TRAF6$^{-/-}$ MEF (Fig. 2*C*).

To further examine the involvement of TRAF6 in IL-25R-mediated NF-κB activation, we compared IL-25R-mediated nuclear accumulation of NF-κB p65 in Flag-IL-25R-expressing WT MEF and TRAF6$^{-/-}$ MEF. Nuclear accumulation of NF-κB p65 was induced by IL-25 stimulation (Fig. 2*D*, *top panel*) or by anti-Flag mAb-mediated IL-25R cross-linking (Fig. 2*D*, *bottom panel*) in Flag-IL-25R-expressing WT MEF. IL-25-mediated or anti-Flag mAb-mediated nuclear accumulation of NF-κB p65 was significantly decreased in Flag-IL-25R-expressing TRAF6$^{-/-}$ MEF (Fig. 2*D*). Taken together, these results indicate that TRAF6 is involved in IL-25R-mediated NF-κB activation.

TRAF6 associates with IL-25R

We then examined whether TRAF6 associates with IL-25R by a coimmunoprecipitation assay. Flag-tagged TRAF6 was expressed with or without *myc*-tagged IL-25R in COS7 cells and the amounts of Flag-tagged TRAF6 in the immunoprecipitates with anti-*myc* mAb was evaluated. As shown in Fig. 3*A*, anti-*myc* mAb coprecipitated Flag-tagged TRAF6. We also performed the immunoprecipitation with anti-Flag mAb and confirmed that *myc*-tagged IL-25R was coimmunoprecipitated with Flag-tagged TRAF6 (Fig. 3*B*). In contrast, *myc*-tagged IL-25R was not coimmunoprecipitated with Flag-tagged TRAF2 or TRAF5 (Fig. 3*B*). These results suggest that TRAF6 but not TRAF2 or TRAF5 can associate with IL-25R and that this association occurs even in the absence of ligand binding. Furthermore, IL-25R-mediated NF-κB activation was attenuated in cells expressing IL-25R E338A, in which TRAF6-binding motif was mutated, compared with that in cells expressing WT IL-25R (Fig. 3*C*). These results suggest that the direct association between IL-25R and TRAF6 is crucial for IL-25-mediated NF-κB activation.

IL-25 induces MAPK activation by a TRAF6-independent mechanism

To determine whether IL-25 activates other intracellular signaling pathways such as MAPK pathways, we next examined the phosphorylation of ERK, JNK, and p38 in Flag-IL-25R-expressing MEF upon stimulation with anti-Flag mAb. The phosphorylation of ERK was markedly induced upon stimulation with anti-Flag mAb at similar levels to that induced by IL-17 or IL-1 stimulation (Fig. 4). The phosphorylation of JNK and p38 was also induced by the stimulation with anti-Flag mAb, although it was weaker than that induced by IL-17 or IL-1 stimulation (Fig. 4). These results indicate that IL-25 activates not only the NF-κB pathway but also ERK, JNK, and p38 pathways. Interestingly, although IL-17- or IL-1-mediated activation of JNK and p38 was impaired in TRAF6$^{-/-}$ MEF (Fig. 4, *lane 3* vs *lane 7* and *lane 4* vs *lane 8*, respectively), IL-25R-mediated activation of ERK, JNK, and p38 was not impaired in TRAF6$^{-/-}$ MEF (Fig. 4, *lane 2* vs *lane 6*). These results indicate that in contrast to IκB-α down-regulation

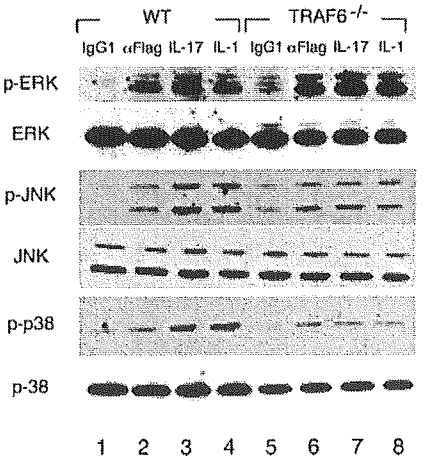

FIGURE 4. IL-25 activates ERK, JNK, and p38 by a TRAF6-independent mechanism. Similar to Fig. 2*C*, WT or TRAF6$^{-/-}$ MEF infected with retrovirus of pMX-Flag-IL-25R-IRES-GFP were incubated with control IgG1, anti-Flag mAb, IL-17, or IL-1 at 37°C for 20 min, and cell lysates were subjected to immunoblotting with anti-phospho-ERK, anti-ERK, anti-phospho-JNK, anti-JNK, anti-phospho-p38, or anti-p38 Ab. Shown are representative blots from four independent experiments.

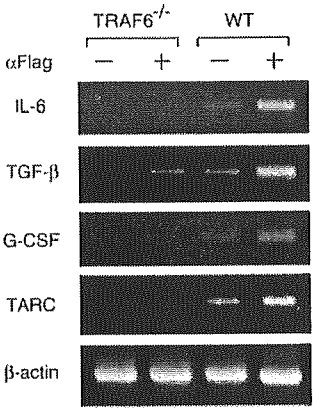

FIGURE 5. IL-25 up-regulates cytokine and chemokine mRNA expression in a TRAF6-dependent manner. WT MEF and TRAF6$^{-/-}$ MEF were infected with retrovirus of pMX-Flag-IL-25R-IRES-GFP as described in Fig. 2*C* and then incubated with anti-Flag mAb or control IgG1 at 37°C for 3 h. Total cellular RNA was prepared, and RT-PCR analysis for IL-6, TGF-β, G-CSF, TARC, and β-actin (as a control) was performed. Shown are representative data of four independent experiments.

and subsequent NF-κB activation (Fig. 2, *B* and *C*), TRAF6-independent pathways mainly contribute to the activation of ERK, JNK, and p38 under IL-25R-mediated signaling.

TRAF6 is involved in IL-25R-mediated gene expression

To determine whether TRAF6 is involved in IL-25R-mediated gene expression, we compared the mRNA induction of IL-6, TGF-β, G-CSF, and TARC in Flag-IL-25R-expressing WT MEF with Flag-IL-25R-expressing TRAF6$^{-/-}$ MEF upon stimulation with anti-Flag mAb. Interestingly, the induction of mRNA expression of IL-6, TGF-β, G-CSF, and TARC by anti-Flag cross-linking was significantly decreased in Flag-IL-25R-expressing TRAF6$^{-/-}$ MEF, compared with that in Flag-IL-25R-expressing WT MEF (Fig. 5). The induction of IL-6, TGF-β, G-CSF, and TARC mRNA was also attenuated in Flag-IL-25R E338A-expressing WT MEF, compared with that in Flag-IL-25R-expressing WT MEF (data not shown). Taken together, these results suggest that TRAF6 plays an important role in the production of cytokines and chemokines upon IL-25R-mediated signaling.

Discussion

In this study, we show that TRAF6 mediates NF-κB activation in IL-25R signaling. We found that IL-25R-mediated signaling induced NF-κB activation (Fig. 2*A*) as well as ERK, JNK, and p38 activation (Fig. 4). We also found that IL-25R-mediated NF-κB activation was down-regulated by the expression of DN TRAF6 but not of DN TRAF2 (Fig. 2*B*). Furthermore, IL-25R-mediated NF-κB activation, but not MAPK activation, was diminished in TRAF6$^{-/-}$ MEF (Figs. 2*C* and 4). In addition, coimmunoprecipitation assay revealed that TRAF6 associated with IL-25R in a ligand-independent manner (Fig. 3, *A* and *B*). Finally, we found that IL-25R-mediated gene expression of IL-6, TGF-β, G-CSF, and TARC was diminished in TRAF6$^{-/-}$ MEF (Fig. 4). Taken together, these results indicate that TRAF6 plays a critical role in IL-25R-mediated NF-κB activation and gene expression.

Our results suggest that TRAF6 directly associates with the cytoplasmic region of IL-25R and induces NF-κB activation upon ligand binding. The TRAF6-binding motif is conserved in the cytoplasmic region of mouse and human IL-25R and we showed the association between IL-25R and TRAF6 even in the absence of ligand binding (Fig. 3, *A* and *B*). We also found that the disruption of the TRAF6-binding motif attenuated IL-25R-mediated NF-κB activation (Fig. 3*C*). In contrast, although there is no TRAF6-binding motif in IL-17R, TRAF6 was coimmunoprecipitated with IL-17R (26) and IL-17-induced NF-κB activation was diminished in TRAF6$^{-/-}$ cells (26) (Fig. 2*C*). Therefore, the mechanisms underlying TRAF6 activation may be different between IL-25R- and IL-17R-mediated signaling.

In contrast, we show that IL-25R-mediated activation of ERK, JNK, and p38 is TRAF6-independent (Fig. 4). We found that IL-25R-mediated ERK, JNK, and p38 activation was similarly observed in WT and TRAF6$^{-/-}$ MEF (Fig. 4). In contrast, we found that IL-17R-mediated JNK and p38 activation was diminished in TRAF6$^{-/-}$ MEF (Fig. 4). Schwandner et al. (26) have also shown that IL-17-induced JNK activation is impaired in TRAF6$^{-/-}$ cells. These results indicate that TRAF6-independent pathways are primarily involved in the activation of JNK and p38 under IL-25R- but not IL-17R-mediated signaling.

The mechanisms by which IL-25 activates these MAPKs have not yet been elucidated. These MAPKs are activated by their specific MAPK kinases: ERK is activated by MEK1 and MEK2, JNK is activated by MAPK kinase (MKK)4 and MKK7, and p38 is activated by MKK3 and MKK6 (28). These MAPK kinases are also activated by various MAPK kinase kinases, such as Raf, TGF-β-activated protein kinase 1, MEK kinase 1, MLK, and apoptosis signal-regulating kinase 1 (28). In preliminary experiments, we found that IL-25R cross-linking modestly induced Raf-1 and MKK3 activation in Flag-IL-25R-expressing cells. However, the induction of Raf-1 and MKK3 activation by IL-25R cross-linking was weaker than that by IL-1 or IL-17. Thus, other kinases may be participated in the activation of these MAPKs under IL-25R signaling. Future studies revealing the signaling cascade of IL-25-induced MAPKs activation especially in the undefined IL-25-responding cells could help the understanding of the physiological importance of MAPKs activation through IL-25R signaling.

Our results also show that IL-25R-mediated signaling induces the production of TARC by a TRAF6-dependent mechanism (Fig. 5). We also found that rIL-25-induced TARC expression in NIH3T3 cells (data not shown). Our findings support the previous report showing that the in vivo administration of IL-25-expressing adenovirus induces the expression of chemokines including TARC in the lung (4). TARC is a specific ligand for CCR4 (29, 30) and induces chemotaxis of T cells, especially of Th2 cells (31, 32). It has also been demonstrated that TARC plays a significant role for the induction of Th2 cell-mediated eosinophil recruitment into the airways in a murine model of asthma (33). We also found that mice that specifically expressed IL-25 in the lung under the control of CC-10 (Clara cell 10-kDa) promoter exhibited the enhanced T cell recruitment into the airways after Ag inhalation (T. Tamachi, Y. Maezawa, K. Ikeda, S.-i. Kagami, M. Hatano, Y. Seto, A. Suto, K. Suzuki, N. Watanabe, Y. Saito, T. Tokuhisa, I. Iwamoto, and H. Nakajima, manuscript in preparation). Therefore, it is suggested that the induction of TARC by IL-25-induced NF-κB activation may be involved in IL-25-mediated allergic inflammation.

IL-25 is expressed in Th2-polarized CD4$^+$ T cells (2) and activated mast cells (34). It has also been reported that in vivo administration of IL-25 promotes the expression of Th2-cell associated cytokines such as IL-4, IL-5, and IL-13 from a non-T/non-B cell population (2, 4). These findings suggest that IL-25 is within the amplification loop of Th2-type immune responses. In this regard, a recent study has demonstrated that APCs such as macrophages and dendritic cells express IL-25R upon IL-4 stimulation (35), suggesting that APCs may be involved in the IL-25-induced Th2-type immune responses. Further investigation is needed to

determine cell populations that respond to IL-25 and trigger Th2-type immune responses in vivo.

In summary, we have demonstrated that TRAF6 is involved in IL-25R-mediated NF-κB activation and gene expression. Because IL-25 is suggested to be involved in Th2 cell-mediated allergic inflammation by inducing Th2 cytokine production from an unidentified non-T/non-B cell population, the elucidation of IL-25R-mediated signaling provides a new tool for the treatment of allergic diseases such as bronchial asthma, atopic rhinitis, and atopic dermatitis.

Acknowledgments

We thank Dr. John D. Shaughnessy, Jr., for providing an expression vector for murine IL-25R; Dr. Toshio Kitamura for expression vector of MPL, pMX-IRES-GFP, and Plat-E cells; and Dr. Hajime Karasuyama for X63 cells, X63-IL-3 cells, and BCMGS neo.

Disclosures

The authors have no financial conflict of interest.

References

1. Lee, J., W. H. Ho, M. Maruoka, R. T. Corpuz, D. T. Baldwin, J. S. Foster, A. D. Goddard, D. G. Yansura, R. L. Vandlen, W. I. Wood, and A. L. Gurney. 2001. IL-17E, a novel proinflammatory ligand for the IL-17 receptor homolog IL-17Rh1. *J. Biol. Chem.* 276: 1660–1664.
2. Fort, M. M., J. Cheung, D. Yen, J. Li, S. M. Zurawski, S. Lo, S. Menon, T. Clifford, B. Hunte, R. Lesley, et al. 2001. IL-25 induces IL-4, IL-5 and IL-13 and Th2-associated pathologies in vivo. *Immunity* 15: 985–995.
3. Pan, G., D. French, W. Mao, M. Maruoka, P. Risser, J. Lee, J. Foster, S. Aggarwal, K. Nicholes, S. Guillet, et al. 2001. Forced expression of murine IL-17E induces growth retardation, jaundice, a Th2-biased response, and multiorgan inflammation in mice. *J. Immunol.* 167: 6559–6567.
4. Hurst, S. D., T. Muchamuel, D. M. Gorman, J. M. Gilbert, T. Clifford, S. Kwan, S. Menon, B. Seymour, C. Jackson, T. T. Kung, et al. 2002. New IL-17 family members promote Th1 or Th2 responses in the lung: in vivo function of the novel cytokine IL-25. *J. Immunol.* 169: 443–453.
5. Aggarwal, S., and A. L. Gurney. 2002. IL-17: prototype member of an emerging cytokine family. *J. Leukocyte Biol.* 71: 1–8.
6. Moseley, T. A., D. R. Haudenschild, L. Rose, and A. H. Reddi. 2003. Interleukin-17 family and IL-17 receptors. *Cytokine Growth Factor Rev.* 14: 155–174.
7. Kolls, J. K., and A. Linden. 2004. Interleukin-17 family members and inflammation. *Immunity* 21: 467–476.
8. Kim, M. R., R. Manoukian, R. Yeh, S. M. Silbiger, D. M. Danilenko, S. Scully, J. Sun, M. L. DeRose, M. Stolina, D. Chang, et al. 2002. Transgenic overexpression of human IL-17E results in eosinophilia, B-lymphocyte hyperplasia, and altered antibody production. *Blood* 100: 2330–2340.
9. Schwarzenberger, P., V. La Russa, A. Miller, P. Ye, W. Huang, A. Zieske, S. Nelson, G. J. Bagby, D. Stoltz, R. L. Mynatt, et al. 1998. IL-17 stimulates granulopoiesis in mice: use of an alternate, novel gene therapy-derived method for in vivo evaluation of cytokines. *J. Immunol.* 161: 6383–6389.
10. Linden, A., H. Hoshino, and M. Laan. 2000. Airway neutrophils and interleukin-17. *Eur. Respir. J.* 15: 973–977.
11. Shi, Y., S. J. Ullrich, J. Zhang, K. Connolly, K. J. Grzegorzewski, M. C. Barber, W. Wang, K. Wathen, V. Hodge, C. L. Fisher, et al. 2000. A novel cytokine receptor-ligand pair: identification, molecular characterization, and in vivo immunomodulatory activity. *J. Biol. Chem.* 275: 19167–19176.
12. Tian, E., J. R. Sawyer, D. A. Largaespada, N. A. Jenkins, N. G. Copeland, and J. D. Shaughnessy, Jr. 2000. Evi27 encodes a novel membrane protein with homology to the IL17 receptor. *Oncogene* 19: 2098–2109.
13. Wajant, H., M. Grell, and P. Scheurich. 1999. TNF receptor associated factors in cytokine signaling. *Cytokine Growth Factor Rev.* 10: 15–26.
14. Bradley, J. R., and J. S. Pober. 2001. Tumor necrosis factor receptor-associated factors (TRAFs). *Oncogene* 20: 6482–6491.
15. Chung, J. Y., Y. C. Park, H. Ye, and H. Wu. 2002. All TRAFs are not created equal: common and distinct molecular mechanisms of TRAF-mediated signal transduction. *J. Cell Sci.* 115: 679–688.
16. Wu, H., and J. R. Arron. 2003. TRAF6, a molecular bridge spanning adaptive immunity, innate immunity and osteoimmunology. *BioEssays* 25: 1096–1105.
17. Ye, H., J. R. Arron, B. Lamothe, M. Cirilli, T. Kobayashi, N. K. Shevde, D. Segal, O. K. Dzivenu, M. Vologodskaia, M. Yim, et al. 2002. Distinct molecular mechanism for initiating TRAF6 signaling. *Nature* 418: 443–447.
18. Takatsuna, H., H. Kato, J. Gohda, T. Akiyama, A. Moriya, Y. Okamoto, Y. Yamagata, M. Otsuka, K. Umezawa, K. Semba, and J. Inoue. 2003. Identification of TIFA as an adapter protein that links tumor necrosis factor receptor-associated factor 6 (TRAF6) to interleukin-1 (IL-1) receptor-associated kinase-1 (IRAK-1) in IL-1 receptor signaling. *J. Biol. Chem.* 278: 12144–12150.
19. Karasuyama, H., and F. Melchers. 1988. Establishment of mouse cell lines which constitutively secrete large quantities of interleukin 2, 3, 4 or 5, using modified cDNA expression vectors. *Eur. J. Immunol.* 18: 97–104.
20. Kobayashi, N., Y. Kadono, A. Naito, K. Matsumoto, T. Yamamoto, S. Tanaka, and J. Inoue. 2001. Segregation of TRAF6-mediated signaling pathways clarifies its role in osteoclastogenesis. *EMBO J.* 20: 1271–1281.
21. Morita, S., T. Kojima, and T. Kitamura. 2000. Plat-E: an efficient and stable system for transient packaging of retroviruses. *Gene Ther.* 7: 1063–1066.
22. Geddis, A. E., H. M. Linden, and K. Kaushansky. 2002. Thrombopoietin: a pan-hematopoietic cytokine. *Cytokine Growth Factor Rev.* 13: 61–73.
23. Ishida, T., S. Mizushima, S. Azuma, N. Kobayashi, T. Tojo, K. Suzuki, S. Aizawa, T. Watanabe, G. Mosialos, E. Kieff, et al. 1996. Identification of TRAF6, a novel tumor necrosis factor receptor-associated factor protein that mediates signaling from an amino-terminal domain of the CD40 cytoplasmic domain. *J. Biol. Chem.* 271: 28745–28748.
24. Suto, A., H. Nakajima, K. Hirose, K. Suzuki, S. Kagami, Y. Seto, A. Hoshimoto, Y. Saito, D. C. Foster, and I. Iwamoto. 2002. Interleukin-21 prevents antigen-induced IgE production by inhibiting germline Cε transcription of IL-4-stimulated B cells. *Blood* 100: 4565–4573.
25. Cao, Z., J. Xiong, M. Takeuchi, T. Kurama, and D. V. Goeddel. 1996. TRAF6 is a signal transducer for interleukin-1. *Nature* 383: 443–446.
26. Schwandner, R., K. Yamaguchi, and Z. Cao. 2000. Requirement of tumor necrosis factor-associated factor (TRAF) 6 in interleukin 17 signal transduction. *J. Exp. Med.* 191: 1233–1239.
27. Shalom-Barak, T., J. Quach, and M. Lotz. 1998. Interleukin-17-induced gene expression in articular chondrocytes is associated with activation of mitogen-activated protein kinases and NF-κB. *J. Biol. Chem.* 273: 27467–27473.
28. Johnson, G. L., H. G. Dohlman, and L. M. Graves. 2005. MAPK kinase kinases (MKKKs) as a target class for small-molecule inhibition to modulate signaling networks and gene expression. *Curr. Opin. Chem. Biol.* 9: 325–331.
29. Imai, T., M. Baba, M. Nishimura, M. Kakizaki, S. Takagi, and O. Yoshie. 1997. The T cell-directed CC chemokine TARC is a highly specific biological ligand for CC chemokine receptor 4. *J. Biol. Chem.* 272: 15036–15042.
30. Imai, T., D. Chantry, C. J. Raport, C. L. Wood, M. Nishimura, R. Godiska, O. Yoshie, and P. W. Gray. 1998. Macrophage-derived chemokine is a functional ligand for the CC chemokine receptor 4. *J. Biol. Chem.* 273: 1764–1768.
31. Bonecchi, R., G. Bianchi, P. P. Bordignon, D. D'Ambrosio, R. Lang, A. Borsatti, S. Sozzani, P. Allavena, P. A. Gray, A. Mantovani, and F. Sinigaglia. 1998. Differential expression of chemokine receptors and chemotactic responsiveness of type 1 T helper cells (Th1s) and Th2s. *J. Exp. Med.* 187: 129–134.
32. Sallusto, F., D. Lenig, C. R. Mackay, and A. Lanzavecchia. 1998. Flexible programs of chemokine receptor expression on human polarized T helper 1 and 2 lymphocytes. *J. Exp. Med.* 187: 875–883.
33. Kawasaki, S., H. Takizawa, H. Yoneyama, T. Nakayama, R. Fujisawa, M. Izumizaki, T. Imai, O. Yoshie, I. Homma, K. Yamamoto, and K. Matsushima. 2001. Intervention of thymus and activation-regulated chemokine attenuates the development of allergic airway inflammation and hyperresponsiveness in mice. *J. Immunol.* 166: 2055–2062.
34. Ikeda, K., H. Nakajima, K. Suzuki, S.-I. Kagami, K. Hirose, A. Suto, Y. Saito, and I. Iwamoto. 2003. Mast cell produce interleukin-25 upon FcεRI-mediated activation. *Blood* 101: 3594–3596.
35. Gratchev, A., J. Kzhyshkowska, K. Duperrier, J. Utical, F. W. Velten, and S. Goerdt. 2004. The receptor for interleukin-17E is induced by Th2 cytokines in antigen-presenting cells. *Scand. J. Immunol.* 60: 233–237.

Murine Plasmacytoid Dendritic Cells Produce IFN-γ upon IL-4 Stimulation[1]

Akira Suto, Hiroshi Nakajima,[2] Naoki Tokumasa, Hiroaki Takatori, Shin-ichiro Kagami, Kotaro Suzuki, and Itsuo Iwamoto

IL-4 plays a key role in inducing IL-4 production in $CD4^+$ T cells, functioning as an important determinant for Th2 cell differentiation. We show here that IL-4 induces IFN-γ production in $B220^+$ plasmacytoid dendritic cells (PDCs). By searching for cell populations that produce IFN-γ upon IL-4 stimulation, we found that PDCs were a major IFN-γ-producing cell upon IL-4 stimulation in wild-type and Rag-$2^{-/-}$ splenocytes. Isolated PDCs, but not $CD11b^+$ DCs or $CD8^+$ DCs, produced IFN-γ upon IL-4 stimulation. In vivo, the depletion of PDCs by anti-Ly6G/C Ab prevented IFN-γ production induced by IL-4 administration. We also found that IL-4 induced IFN-γ production, but not IL-12 or IFN-α production, in PDCs and also strongly enhanced CpG oligodeoxynucleotide-induced IFN-γ production, but not CpG oligodeoxynucleotide-induced IL-12 or IFN-α production. However, IL-4 did not induce IFN-γ production in Stat$6^{-/-}$ PDCs. Moreover, IL-4 induced Stat4 expression in PDCs through a Stat6-dependent mechanism, and only the Stat4-expressing PDCs produced IFN-γ. Furthermore, IL-4 did not induce IFN-γ production in Stat$4^{-/-}$ PDCs. These results indicate that PDCs preferentially produce IFN-γ upon IL-4 stimulation by Stat6- and Stat4-dependent mechanisms. *The Journal of Immunology,* **2005, 175: 5681–5689.**

Cytokine environment is critical for the differentiation and commitment of immune cells. For example, IL-4, a representative Th2 cytokine, induces further Th2 cell differentiation, whereas a Th1 cytokine IFN-γ in coordination with IL-12 induces Th1 cell differentiation (1–3). Although these positive feedback mechanisms are essential for the profound differentiation of Th cells, the immune system also has a number of intrinsic and extrinsic machinery to antagonize the excessive differentiation of immune cells (4, 5).

Dendritic cells (DCs)[3] are a migratory group of bone marrow-derived leukocytes with at least three subtypes in mouse spleen: $CD8^+$ DCs, $CD11b^+$ DCs, and $B220^+$ DCs ("plasmacytoid DCs") (PDCs) (6, 7). Although $CD8^+$ DCs and $CD11b^+$ DCs express high levels of MHC class II molecules and costimulatory molecules such as CD80 and induce T cell proliferation, PDCs express MHC class II molecules at very low levels, do not express CD80, and fail to stimulate T cell proliferation (8, 9). These findings suggest that PDCs are immature DCs with a weak ability as APCs. On the other hand, PDCs localize in the T cell zone of lymphoid tissues and produce a large amount of type I IFNs upon bacterial or viral infection (10–12). Therefore, it is suggested that PDCs play a key role in innate immune responses.

Recently, a number of experiments have suggested that innate immune responses contribute significant polarizing influences on Th differentiation (13). The global view is that TLR activation of APCs such as DCs induces cytokine production that favors Th1-type immune responses and prevents the development of deleterious Th2 responses (13). On the other hand, a recent study has shown that PDCs inhibit Th2 responses even in the absence of TLR signaling (14). However, the role of PDCs in Th differentiation is still largely unknown.

In this study, by searching for cell populations that produce IFN-γ upon IL-4 stimulation, we found that PDCs were a major IFN-γ-producing cell upon IL-4 stimulation and that IL-4 preferentially induced IFN-γ production in PDCs by a Stat6-dependent mechanism. We also found that IL-4 induced Stat4 expression in PDCs through a Stat6-dependent mechanism and that only the Stat4-expressing PDCs produced IFN-γ. Furthermore, we found that Stat4-deficient PDCs did not produce IFN-γ upon IL-4 stimulation. Our results highlight a unique function of IL-4-induced IFN-γ production in PDCs in the immune regulation of cytokine networks.

Materials and Methods

Mice

BALB/c mice were purchased from Charles River Laboratories. Stat6-deficient (Stat$6^{-/-}$) mice (15) and Rag-$2^{-/-}$ mice were backcrossed for more than eight generations onto BALB/c mice. Stat$4^{-/-}$ mice on a BALB/c background were purchased from The Jackson Laboratory. OVA-specific DO11.10 TCR transgenic (DO11.10^+) mice (16) were backcrossed over 10 generations onto BALB/c mice. All mice were housed in microisolator cages under specific pathogen-free conditions and all experiments were performed according to the guidelines of Chiba University.

Reagents

Mouse IL-2, IL-4, IL-7, IL-9, IL-13, and IL-15 were purchased from PeproTech. Phosphorothioate-stabilized CpG oligodeoxynucleotide (ODN) 1668 (TCCATGACGTTCCTGATGCT) was purchased from Hokkaido System Science.

Department of Allergy and Clinical Immunology, Graduate School of Medicine, Chiba University, Chiba, Japan

Received for publication January 19, 2005. Accepted for publication August 15, 2005.

The costs of publication of this article were defrayed in part by the payment of page charges. This article must therefore be hereby marked *advertisement* in accordance with 18 U.S.C. Section 1734 solely to indicate this fact.

[1] This work was supported in part by grants from Special Coordination Funds for Promoting Science and Technology from the Ministry of Education, Culture, Sports, Science and Technology, the Japanese Government.

[2] Address correspondence and reprint requests to Dr. Hiroshi Nakajima, Department of Allergy and Clinical Immunology, Graduate School of Medicine, Chiba University, 1-8-1 Inohana, Chiba City, Chiba 260-8670, Japan. E-mail address: nakajimh@faculty.chiba-u.jp

[3] Abbreviations used in this paper: DC, dendritic cell; PDC, plasmacytoid DC; ODN, oligodeoxynucleotide; WT, wild type.

0022-1767/05/$02.00

Flow cytometric analysis

Cells were stained and analyzed on a FACSCalibur (BD Biosciences) using CellQuest software. The following Abs were purchased from BD Pharmingen: anti-CD4 FITC, PE (H129.19), anti-CD8 FITC, PE (53-6.7), anti-B220 FITC, PE, allophycocyanin, PerCP, biotin (RA3-6B2), anti-CD3 PE (145-2C11), anti-CD19 PE (ID3), anti-CD11b (Mac-1) PE (M1/70), anti-CD11c FITC (HL3), anti-Ly6G/C PE (RB6-8C5), anti-erythroid PE (TER-119), anti-pan NK PE (DX5), anti-CD80 PE (16-10A1), anti-CD86 PE (GL-1), and anti-I-A^d PE (AMS-32.1). Before staining, FcRs were blocked with anti-CD16/32 Ab (2.4G2; BD Pharmingen). Negative controls consisted of isotype-matched, directly conjugated, nonspecific Abs (BD Pharmingen).

Isolation of DC subtypes

Splenic DCs were prepared using OptiPrep (Axis Shield) according to the manufacturer's instructions. In brief, spleens were cut into small fragments and then digested with collagenase A (0.5 mg/ml; Roche) for 10 min at 37°C with continuous agitation. Digested fragments were filtered through a stainless steel sieve, and cells were resuspended in 3 ml of HBSS and then mixed with 1 ml of OptiPrep to make 15% iodixanol solution (density 1.085 g/ml). Cell suspension was overlaid with 5 ml of 12% iodixanol solution (density 1.069 g/ml) and subsequently with 3 ml of HBSS. Low-density cells were collected by centrifugation at 600 × *g* for 15 min at room temperature. Low-density cells were stained with anti-CD11c FITC and FITC-stained cells were positively collected using anti-FITC microbeads (Miltenyi Biotec), according to the manufacturer's instructions. The resultant cells were routinely >95% pure $CD11c^+$ cells by FACS analysis.

To isolate PDCs, low-density cells were prepared from wild-type (WT), $Stat6^{-/-}$ splenocytes, or $Stat4^{-/-}$ splenocytes and then stained with a mixture of PE-labeled Abs to CD3, CD19, CD11b, DX5, and TER-119. After PE-stained cells were depleted using anti-PE microbeads (Miltenyi Biotec), cells in flow-through were stained with anti-B220 biotin and subsequently $B220^+$ cells were positively collected using streptavidin microbeads (Miltenyi Biotec). Alternatively, PDCs were purified using a PDC isolation kit according to the manufacturer's instructions (Miltenyi Biotec). In both cases, the resultant cells were >95% pure $B220^+CD19^-$ cells by FACS analysis.

For $CD11b^+$ DCs purification, low-density cells were prepared from WT splenocytes and stained with a mixture of PE-labeled Abs to CD3, B220, DX5, TER-119, and CD8. After PE-stained cells were depleted using anti-PE microbeads, cells in flow-through were stained with anti-CD11c FITC and $CD11c^+$ cells were positively collected using anti-FITC microbeads. The resultant cells were routinely >95% pure $CD11b^+CD8^-CD11c^+$ cells by FACS analysis.

For $CD8^+$ DCs purification, low-density cells were prepared from WT splenocytes and stained with a mixture of PE-labeled Abs against CD3, B220, DX5, TER-119, and CD11b and PE-stained cells were depleted using anti-PE microbeads. Cells in flow-through were stained with anti-CD11c FITC and $CD11c^+$ cells were positively collected using anti-FITC microbeads. The resultant cells were routinely >95% pure $CD11b^-CD8^+CD11c^+$ cells by FACS analysis.

Cell culture

Isolated PDCs, $CD11b^+$ DCs, or $CD8^+$ DCs were cultured (5×10^5/ml) in RPMI 1640 medium supplemented with 10% heat-inactivated FCS, 50 μM 2-ME, 2 mM L-glutamine, and antibiotics (complete RPMI 1640 medium) at 37°C for 72 h in the presence or in the absence of IL-4 (20 ng/ml). In some experiments, PDCs were stimulated with CpG ODN (10 μg/ml) for 48 or 72 h. PDCs were also stimulated with IL-2, IL-7, IL-9, IL-13, or IL-15 (20 ng/ml each) for 72 h to determine whether these cytokines induce IFN-γ production from PDCs. In other experiments, anti-IL-12 (p40/p70) Ab (10 μg/ml, clone C17.8; BD Pharmingen), anti-IL-2R β-chain Ab (10 μg/ml, clone TM-β1; BD Pharmingen), or anti-IL-18 Ab (5 μg/ml, clone 93-10C; MBL) was added to neutralize IL-12, IL-2 and IL-15, or IL-18, respectively. A mixture of anti-murine IFN-α Ab (20 μg/ml, clone 4EA1) (17), anti-murine IFN-β Ab (20 μg/ml, clone 7DF3) (17), and anti-type I IFN receptor antisera (10 μg/ml, R&D Systems) was used to neutralize type I IFNs.

ELISAs

The amounts of IFN-γ and IL-12 in the culture supernatant were measured by the enzyme immunoassay using murine IFN-γ and IL-12 (p70) ELISA kits from BD Pharmingen. The amounts of IFN-α in the culture supernatant were measured by an IFN-α ELISA kit from PBL. The assays were performed in duplicate according to the manufacturers' instruction. The minimum significant values of these assays were 31.3 pg/ml IFN-γ, 62.5 pg/ml IL-12, and 12.5 pg/ml IFN-α.

Intracellular staining for IFN-γ

Cells were stimulated with IL-4 (20 ng/ml) in the complete RPMI 1640 medium for the indicated periods (48 or 72 h). Monensin (2 μM; Sigma-Aldrich) was added for final 4 h to prevent cytokine release. After surface staining, cells were fixed with IC FIX (BioSource International), permeabilized with IC PERM (BioSource International), and stained with anti-IFN-γ allophycocyanin (XMG1.2; BD Pharmingen) as described previously (18).

Intracellular Stat4 staining

Intracellular staining for Stat4 was performed as described elsewhere (19) with minor modifications. In brief, isolated PDCs from WT splenocytes or $Stat6^{-/-}$ splenocytes were cultured for 48 h in the presence or in the absence of IL-4 (20 ng/ml). Cells were harvested, washed with PBS, fixed with IC FIX, and permeabilized with 90% methanol and subsequently with IC PERM. Cells were then incubated with anti-Stat4 Ab (Zymed) or control rabbit IgG (Serotec) for 30 min at room temperature. After washing, cells were incubated with Alexa Fluor 647-conjugated anti-rabbit IgG Ab (Molecular Probes) and analyzed on a FACSCalibur. In the case of double

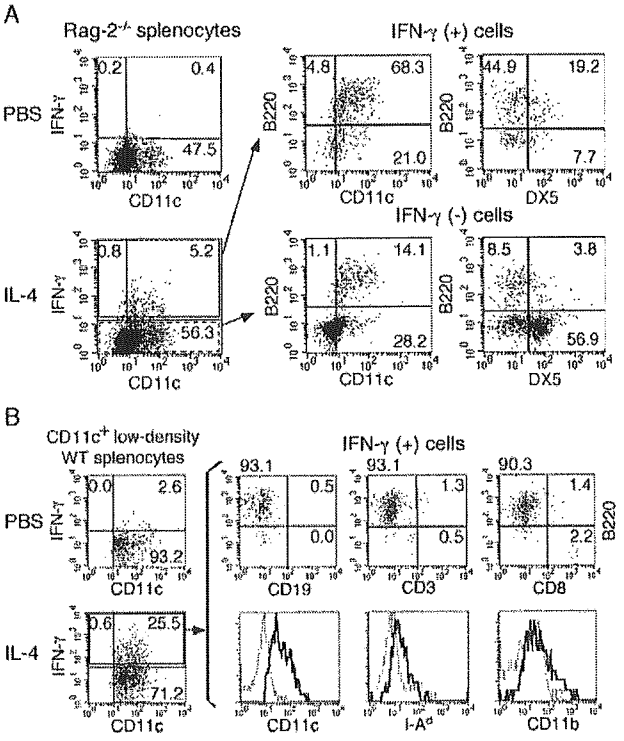

FIGURE 1. $B220^+$ PDCs produce IFN-γ upon IL-4 stimulation. *A*, Splenocytes from Rag-$2^{-/-}$ mice were cultured with or without IL-4 (20 ng/ml) for 3 days with monensin added for the final 4 h. After cells were stained with anti-B220 and either anti-CD11c or anti-DX5, intracellular staining for IFN-γ was performed. Representative FACS profiles of anti-CD11c vs anti-IFN-γ staining (*left panels*) and anti-CD11c vs anti-B220 or anti-DX5 vs anti-B220 staining gating on either $IFN\text{-}\gamma^+$ cells or $IFN\text{-}\gamma^-$ cells (*right panels*) are shown. *B*, $CD11c^+$ low-density splenocytes were isolated from WT mice as described in the *Materials and Methods*. Cells were then cultured with or without IL-4 for 3 days and analyzed for the expression of CD11c, B220, CD19, CD8, CD11b, Ly6G/C, and I-A^d together with the intracellular IFN-γ. Shown are representative FACS profiles of anti-CD11c vs anti-IFN-γ staining from four independent experiments (*left panels*). Representative FACS profiles of anti-CD19 vs anti-B220, anti-CD3 vs anti-B220, and anti-CD8 vs anti-B220 staining on $IFN\text{-}\gamma^+$ cells, as well as histograms for anti-Ly6G/C, anti-CD11b, and anti-I-A^d staining on $IFN\text{-}\gamma^+$ cells are shown in the *right panels*. Dashed lines indicate the staining with isotype-matched control Abs.

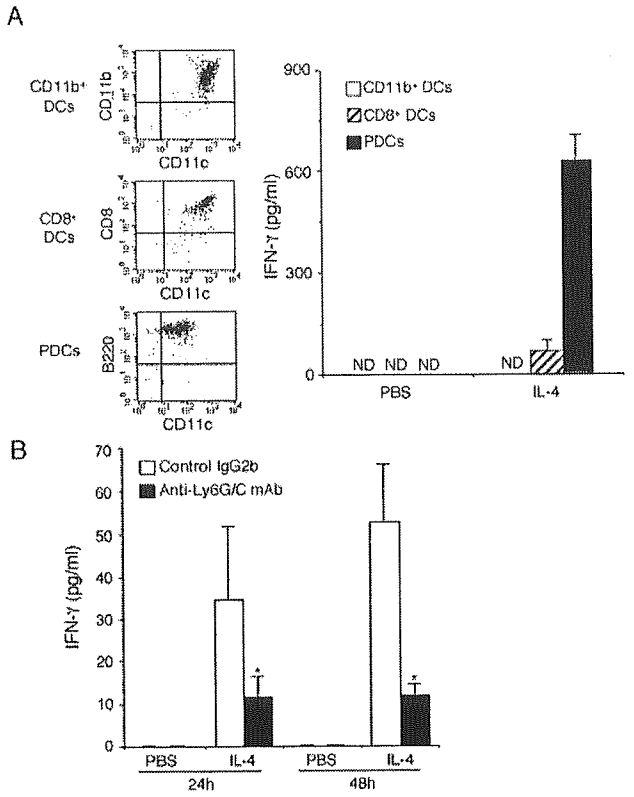

FIGURE 2. PDCs but not CD11b$^+$ or CD8$^+$ DCs produce IFN-γ upon IL-4 stimulation. *A*, PDCs, CD11b$^+$ DCs, and CD8$^+$ DCs were prepared from WT splenocytes as described in *Materials and Methods*. Each DC subtype was cultured with or without IL-4 for 3 days, and the amounts of IFN-γ in the supernatants were measured by ELISA. Representative FACS profiles of isolated each DC subtype are shown in the *left panels*. Data are means ± SD from four independent experiments. ND = not detectable. *B*, PDCs produce IFN-γ upon IL-4 stimulation in vivo. Rag-2$^{-/-}$ mice were injected i.p. with anti-Ly6G/C Ab (500 μg/mouse) or rat IgG2b (as a control). Twenty-four hours later, rIL-4 (10 μg/mouse) or saline (as a control) was injected i.v. in the retro-orbital vein of mice. The levels of IFN-γ in the serum were determined by ELISA at 24 and 48 h after IL-4 injection. Data are means ± SD for four mice in each group. ND, not detectable. *, Significantly different from the mean value of the corresponding control response (control IgG2b); $p < 0.01$.

intracellular staining for Stat4 and IFN-γ, FITC-conjugated anti-rabbit IgG Ab (Zymed) was used as a second Ab.

RT-PCR analysis

Total cellular RNA was prepared and RT-PCR analysis was performed as described previously (20). The primer pairs for Stat4 were 5′-CTTGGGT GGACCAATCTGAA-3′ and 5′-TGGTCTTGAGACTTCGCACG-3′. The primer pairs for GATA3 and T-bet were described elsewhere (21). RT-PCR for β-actin was performed as a control. All PCR amplifications were performed at least three times with multiple sets of experimental RNAs.

Taqman PCR analysis

The expression levels of Stat4 mRNA were determined by real-time PCR using a standard protocol on ABI PRISM 7000 instrument (Applied Biosystems). PCR primers and fluorogenic probes for Stat4, T-bet, and GATA3 were described previously (22). The levels of Stat4 mRNA were normalized to the levels of GAPDH mRNA (Applied Biosystems).

Effect of in vivo depletion of PDCs on IFN-γ production induced by IL-4 administration

To deplete PDCs in vivo, anti-Ly6G/C Ab (500 μg/mouse; BD Pharmingen) was injected i.p. to Rag-2$^{-/-}$ mice as described previously (12). As a control, purified rat IgG2b (BD Pharmingen) was injected to Rag-2$^{-/-}$ mice. In some experiments, 120G8 Ab (500 μg/mouse; a gift from Drs. G. Trinchieri and D. La Face, Schering-Plough Research Institute, Dardilly, France) (23) was injected to Rag-2$^{-/-}$ mice to deplete PDCs. Twenty-four hours later, rIL-4 (10 μg/mouse) or saline (as a control) was injected i.v. in the retro-orbital vein of the mice. The levels of IFN-γ in sera were determined by ELISA using a highly sensitive mouse IFN-γ ELISA kit (AN-18; BD Pharmingen) at 24 and 48 h after IL-4 injection. The minimum significant value of this assay was 3 pg/ml IFN-γ.

Th1 and Th2 cell differentiation

Splenic CD4$^+$ T cells from DO11.10$^+$ mice were purified (>90% pure by flow cytometry) using T cell enrichment columns (R&D Systems) and stimulated with plate-bound anti-CD3ε mAb (5 μg/ml, clone 145-2C11; BD Pharmingen) plus anti-CD28 mAb (5 μg/ml, clone 37.51; BD Pharmingen) at 37°C for 48 h in the presence of IL-12 (7.5 ng/ml; R&D Systems) (Th1 condition) or IL-4 (15 ng/ml; R&D Systems) and anti-IFN-γ mAb (15 μg/ml, clone XMG1.2; BD Pharmingen) (Th2 condition) as described previously (18).

Data analysis

Data are summarized as mean ± SD. The statistical analysis of the results was performed by the unpaired *t* test. Values of $p < 0.05$ were considered significant.

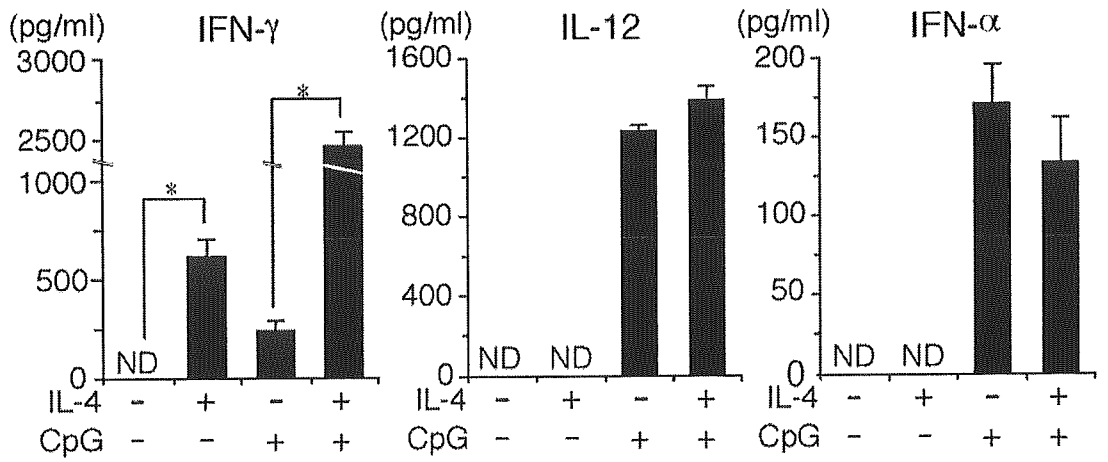

FIGURE 3. IL-4 induces IFN-γ but not IL-12 or IFN-α production in PDCs. Isolated PDCs from WT splenocytes were cultured with IL-4 (20 ng/ml) and/or CpG ODN (10 μg/ml) for 3 days, and the amounts of IFN-γ, IL-12, and IFN-α in the supernatants were measured by ELISA. Data are means ± SD from four independent experiments. ND, not detectable. *, $p < 0.001$.

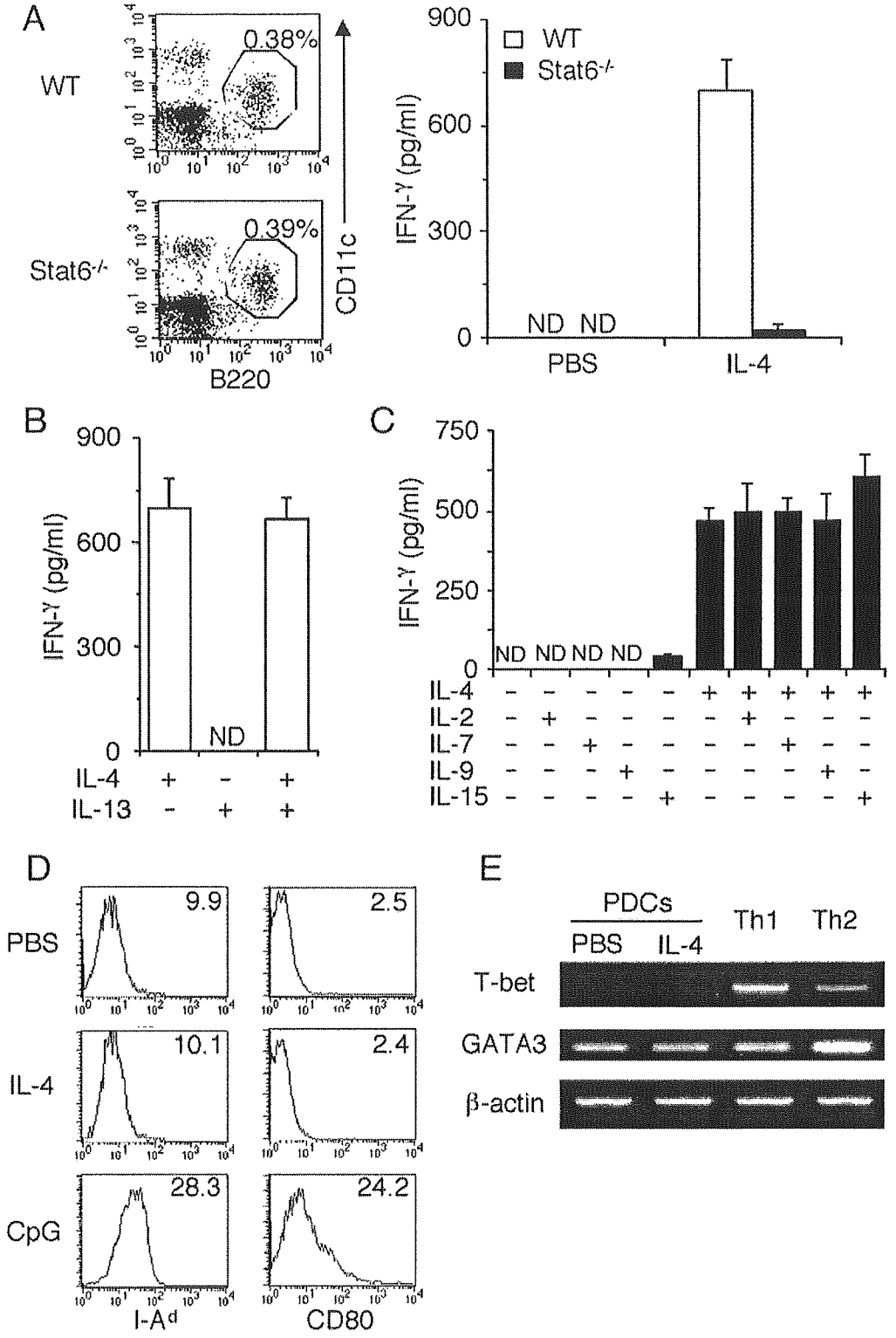

FIGURE 4. IL-4 induces IFN-γ production in PDCs by a Stat6-dependent mechanism. *A*, Stat6 is essential for IL-4-induced IFN-γ production in PDCs. Representative anti-B220 vs anti-CD11c staining on $CD3^-CD11b^-CD19^-DX5^-TER\text{-}119^-$ splenocytes from WT mice and $Stat6^{-/-}$ mice are shown in the *left panels* ($n = 6$ mice for each genotype), indicating normal development of PDCs in $Stat6^{-/-}$ mice. Isolated PDCs from WT splenocytes or $Stat6^{-/-}$ splenocytes were cultured with or without IL-4 for 3 days, and the amounts of IFN-γ in the supernatants were measured by ELISA. Data are means ± SD from four independent experiments. *B*, IL-13 does not induce IFN-γ production in PDCs. Isolated PDCs from WT splenocytes were cultured with IL-4 and/or IL-13 (20 ng/ml) for 3 days, and the amounts of IFN-γ in the supernatants were measured by ELISA. Data are means ± SD from four independent experiments. ND, not detectable. *C*, Other γc-dependent cytokines do not enhance IL-4-induced IFN-γ production from PDCs. Isolated PDCs from WT splenocytes were cultured with IL-2 (20 ng/ml), IL-7 (20 ng/ml), IL-9 (20 ng/ml), or IL-15 (20 ng/ml) in the presence or in the absence of IL-4 (20 ng/ml) for 3 days, and the amounts of IFN-γ in the supernatants were measured by ELISA. Data are means ± SD from four independent (*Figure legend continues*)

Results

$B220^+$ PDCs produce IFN-γ upon IL-4 stimulation

To examine the negative-feedback regulation of cytokine networks, we searched for cell populations that produce IFN-γ upon IL-4 stimulation. We found that ~5% of IL-4-stimulated Rag-$2^{-/-}$ splenocytes became positive for intracellular IFN-γ staining (Fig. 1*A*, *left panels*). Multicolor FACS analyses revealed that the majority of IL-4-induced, IFN-γ-producing cells expressed CD11c at low levels, expressed B220 at high levels, but lacked the expression of DX5 (Fig. 1*A*, *right panels*). In contrast, the majority of IFN-γ-nonproducing cells in IL-4-stimulated Rag-$2^{-/-}$ splenocytes were positive for DX5 but negative for B220 (Fig. 1*A*), suggesting that these IFN-γ-nonproducing cells are NK cells.

To further characterize cell populations that produce IFN-γ upon IL-4 stimulation, $CD11c^+$ low-density splenocytes were isolated from WT mice and then stimulated with IL-4. Again, the majority of IL-4-induced, IFN-γ-producing cells expressed B220 at high levels and expressed CD11c at low levels (Fig. 1*B*). IFN-γ-producing cells were also positive for anti-Ly6G/C staining (Fig. 1*B*). Moreover, IFN-γ-producing cells expressed class II MHC molecules ($I\text{-}A^d$) at very low levels but lacked the expression of CD19, CD3, CD8, and CD11b (Fig. 1*B*). These results suggest that the IL-4-induced, IFN-γ-producing cells are very similar to type I IFN-producing PDCs (10–12).

PDCs but not $CD11b^+$ DC or $CD8^+$ DCs produce IFN-γ upon IL-4 stimulation

To determine whether PDCs specifically produce IFN-γ upon IL-4 stimulation, isolated PDCs, $CD11b^+$ DCs, and $CD8^+$ DCs were examined for their ability of IFN-γ production upon IL-4 stimulation. Consistent with the data obtained by intracellular IFN-γ staining (Fig. 1), isolated PDCs produced a considerable amount of IFN-γ upon IL-4 stimulation (625.5 ± 79.9 pg/ml, means ± SD, $n = 4$) (Fig. 2*A*). On the other hand, IL-4-stimulated $CD8^+$ DCs produced little IFN-γ (74.3 ± 32.2 pg/ml, $n = 4$) and IL-4-stimulated $CD11b^+$ DCs did not produce IFN-γ (Fig. 2*A*). Together with the data shown in Fig. 1, these results indicate that among DC subtypes, PDCs specifically produce IFN-γ upon IL-4 stimulation.

We also examined whether PDCs produced IFN-γ upon IL-4 stimulation in vivo. As shown in Fig. 2*B*, when rIL-4 was administered i.v. to Rag-$2^{-/-}$ mice, a considerable amount of IFN-γ was detected in the serum after 24 and 48 h. Importantly, the depletion of PDCs with preinjection of anti-Ly6G/C Ab significantly decreased the IL-4-induced IFN-γ production ($n = 4$ mice, $p < 0.01$) (Fig. 2*B*). A similar trend was observed with 120G8 Ab, which depletes PDCs more specifically (23), although statistical significance was not achieved due to the limited number of mice examined (data not shown). These results suggest that PDCs produce IFN-γ upon IL-4 stimulation in vivo.

IL-4 preferentially induces IFN-γ production in PDCs

PDCs have been identified as a potent producer of IFN-α and IL-12 upon viral or bacterial infection (8–12). Therefore, we examined whether IL-4-induced IFN-α and IL-12 production in isolated PDCs. However, IL-4 did not induce the production of IFN-α or IL-12 (p70) in PDCs ($n = 4$) (Fig. 3). In contrast, PDCs produced considerable amounts of IFN-γ, IFN-α, and IL-12 upon CpG ODN stimulation, a potent stimulator of PDCs through TLR9 (24, 25) (Fig. 3). Furthermore, IL-4 strikingly enhanced CpG ODN-induced IFN-γ production ~10-fold but not CpG ODN-induced IFN-α or IL-12 production in PDCs ($n = 4$, $p < 0.001$) (Fig. 3). These results indicate that IL-4 preferentially induces IFN-γ production in PDCs.

IL-4 induces IFN-γ production in PDCs by a Stat6-dependent mechanism

It is well established that IL-4 uses Stat6 as a signaling molecule (26). Therefore, we next studied whether Stat6 was required for IL-4-induced IFN-γ production in PDCs using Stat6-deficient (Stat6$^{-/-}$) mice. The number of PDCs ($CD19^-B220^+CD11c^{low}$ cells) in spleen was similar between Stat6$^{-/-}$ mice and WT mice (Fig. 4*A*), suggesting that Stat6 is not essential for the development of PDCs. However, when isolated PDCs were stimulated with IL-4, WT PDCs but not Stat6$^{-/-}$ PDCs produced IFN-γ (Fig. 4*A*). On the other hand, CpG ODN-induced IFN-γ production was similarly observed between WT PDCs and Stat6$^{-/-}$ PDCs (data not shown). These results indicate that among signaling molecules under IL-4, Stat6 is essential for IFN-γ production in PDCs. We also examined the effect of IL-13, which shares type II IL-4R with IL-4 and activates Stat6 (26), on IFN-γ production in PDCs. However, IL-13 did not induce IFN-γ production in PDCs (Fig. 4*B*) nor enhance IL-4-induced IFN-γ production in PDCs (Fig. 4*B*), suggesting that type I IL-4R but not type II IL-4R is involved in IL-4-induced IFN-γ production in PDCs. Moreover, another representative Th2 cytokine, IL-5, did not induce IFN-γ production nor enhance IL-4-induced IFN-γ production in PDCs (data not shown).

Other γc-dependent cytokines do not induce IFN-γ production nor enhance IL-4-induced IFN-γ production in PDCs

To determine whether other γc-dependent cytokines induce IFN-γ production in PDCs, isolated PDCs were stimulated with IL-2, IL-7, IL-9, and IL-15 in the presence or in the absence of IL-4 for 3 days. As shown in Fig. 4*C*, none of γc-dependent cytokines, except for IL-4 induced IFN-γ production in PDCs (Fig. 4*C*). In addition, none of them significantly enhanced IFN-γ production in IL-4-stimulated PDCs (Fig. 4*C*).

IL-4 does not alter the maturation state of PDCs

It has been shown that the ability of DCs for cytokine production depends on their maturation state (27, 28). We then examined whether IL-4 changed the maturation state of PDCs and thus induced IFN-γ-producing ability. Consistent with previous reports (8–12), isolated PDCs expressed $I\text{-}A^d$ at very low levels, and lacked the expression of CD80 (Fig. 4*D*) and CD86 (data not shown). IL-4 did not alter the expression levels of $I\text{-}A^d$, CD80, and CD86 of PDCs (Fig. 4*D* and data not shown). In contrast, when PDCs were stimulated with CpG ODN, the expression levels of $I\text{-}A^d$ and CD80 were significantly increased (Fig. 4*D*). In addition,

experiments. ND, not detectable. *D*, IL-4 does not alter the maturation state of PDCs. Isolated PDCs from WT splenocytes were cultured with IL-4 (20 ng/ml) or CpG ODN (10 μg/ml) for 48 h, and the levels of $I\text{-}A^d$ and CD80 on PDCs were analyzed by FACS. Shown are representative histograms, and the mean fluorescent intensities for anti-$I\text{-}A^d$ and anti-CD80 staining on live cells (propidium iodide $(PI)^-$ cells) from four independent experiments. Forty-three percent of PDCs could survive in the presence of IL-4, whereas 69% of PDCs could survive in the presence of CpG ODN (data not shown). *E*, T-bet is not induced by IL-4 in PDCs. Isolated PDCs from WT splenocytes were cultured with or without IL-4 (20 ng/ml) for 16 h. As controls, Th1-polarized cells or Th2-polarized cells were prepared from DO11.10 TCR transgenic mice as described in the *Materials and Methods*. Shown are representative data of RT-PCR analysis for T-bet, GATA3, and β-actin mRNA from four independent experiments.

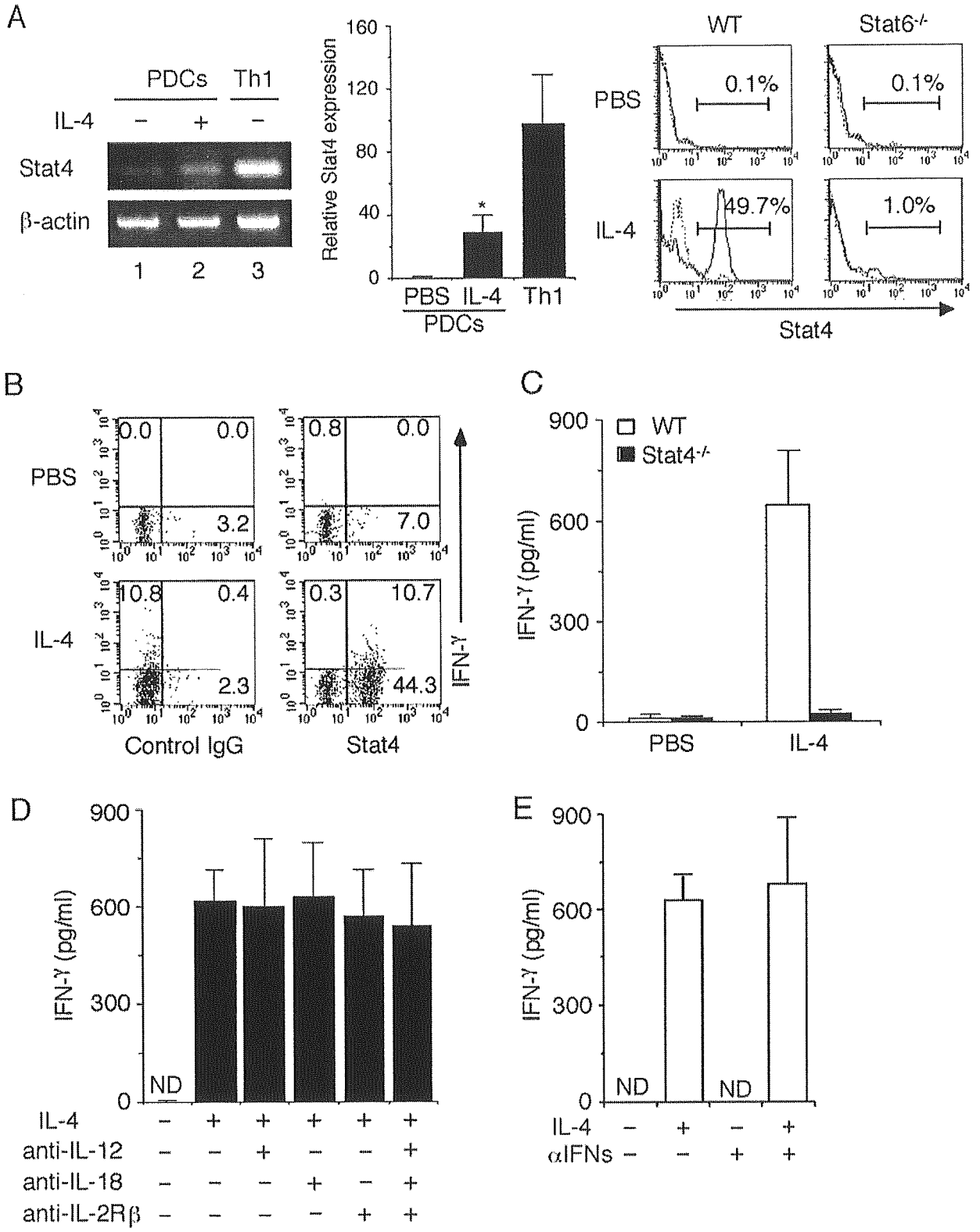

FIGURE 5. IL-4 induces Stat4 expression in PDCs by a Stat6-dependent mechanism. *A*, Isolated PDCs from WT splenocytes were cultured with or without IL-4 (20 ng/ml) for 16 h. As s control for Stat4-expressing cells, Th1-polarized cells were prepared from DO10^{+} mice as described previously (15). Shown are representative data of RT-PCR analysis for Stat4 and β-actin mRNA from four independent experiments (*left panels*). Taqman PCR analysis for Stat4 and GAPDH (as a control) mRNA was performed, and the levels of Stat4 mRNA were normalized to the levels of GAPDH mRNA (*middle panel*). Data are means ± SD from four independent experiments. *, Significantly different from the mean value of control response (PBS); $p < 0.01$. Isolated PDCs from WT splenocytes or Stat6$^{-/-}$ splenocytes were stimulated with or without IL-4 (20 ng/ml) for 48 h, and the expression levels of Stat4 were evaluated by intracellular staining. Shown are representative FACS profiles from four independent experiments (*right panels*). *B*, IL-4-induced, Stat4-expressing PDCs produce IFN-γ. Isolated PDCs from WT splenocytes were cultured with or without IL-4 (20 ng/ml) for 48 h. Intracellular (*Figure legend continues*)